ABSTRACT

Human Kinematic Responses to Riding on a Mechanical Horse Simulating Hippotherapy

Cody R. Barrett, M.S.B.M.E.

Co-Chairperson: Brian Garner, Ph.D
Co-Chairperson: Jonathan Rylander, Ph.D.

Hippotherapy is the use of horseback riding as a form of therapy for a variety of disabilities such as cerebral palsy, multiple sclerosis, and autism. It is also known that hippotherapy can be beneficial for stroke patients and for people suffering lower back pain. Studies have shown that horses' walking patterns exhibit similarities to those of normal human gait, and can have positive effects on people with disabilities or injuries. The aim of this study was to measure and analyze the human body motion responses produced by non-disabled riders of a mechanical horse-riding simulator (MHS) that was developed at Baylor University. In addition, pre and post-test measures were analyzed to compare the after-effects of riding. During riding, the healthy riders' trunk motions tracked closely with the mechanical horse motion in all three anatomical planes. Balance tests showed that the riders, on average, decreased sway in the frontal and sagittal planes after riding, but increased yaw in the transverse plane. The results that the MHS can produce similar kinematic effects to that of a horse should be of interest for the purpose of broadening accessibility to the potential benefits of equine-like motion therapy.

Human Kinematic Responses to Riding a Mechanical Horse Simulating Hippotherapy

by

Cody Barrett, B.S.M.E.

A Thesis

Approved by the Department of Mechanical Engineering

_____

Kenneth Van Treuren, Ph.D., Interim Chairperson

Submitted to the Graduate Faculty of
Baylor University in Partial Fulfillment of the
Requirements for the Degree
of

Master of Science in Biomedical Engineering

Approved by the Thesis Committee

_____

Brian Garner, Ph.D., Chairperson

_____

Jonathan Rylander, Ph.D.

_____

Jaeho Shim, Ph.D.

Accepted by the Graduate School

August 2018

_____

J. Larry Lyon, Ph.D., Dean

Page bearing signatures is kept on file in the Graduate School.

TABLE OF CONTENTS

LIST OF FIGURES

LIST OF TABLES

ACKNOWLEDGMENTS

I would like to thank my committee, Dr. Garner, Dr. Rylander, and Dr. Shim for their support over the past two years. I would also like to thank Dr. Adam Goodworth for helping shape this project during his sabbatical at Baylor. Finally, I would like to thank Jenny Tavares and Tyler Jost for assisting with data collections and analysis methods.

DEDICATION

To my loving family. Without you, none of this would be possible.

CHAPTER ONE

Introduction

Disabilities such as cerebral palsy, multiple sclerosis, and muscular dystrophy affect millions of children in the United States daily. These disabilities have the potential to affect muscle strength and control, leading to difficulties with everyday tasks such as walking. There are multiple therapeutic methods to help such individuals maintain or improve motor control, and one of the more interesting methods is called hippotherapy or equine-assisted therapy. Hippotherapy is a treatment strategy that involves time riding on horseback, under the supervision and guidance of a certified therapist. It can provide beneficial effects for children with disabilities [1–4]. However, accessibility to therapy with a horse may be limited by such factors as geographical location, weather, allergies, fear of horses, cost, and safety concerns for those with more severe disabilities. Inspired by the desire to provide a complementary tool to make equine motion therapy more accessible, a mechanical horse-riding simulator (MHS) has been developed at Baylor University. Through the use of a single motor powered by a regular 120V outlet, the MHS can closely replicate the motion of a real horse in all six degrees of freedom [5].

The aim of this study was to measure and analyze the human body responses produced by non-disabled riders in response to motion imparted by the mechanical horse-riding simulator (MHS). Pre and post-test measures of common balance assessments were also analyzed to compare the effects resulting after riding. EMG and motion capture data were used to evaluate kinematic and muscular effects of riding.

Common Disabilities

It is estimated that about 54 million people in the United States have some type of disability [6]. Even more importantly, about 35 million people are considered to have a severe disability. These numbers indicate that 22% of adults in the US have some form of disability and 12% are severe [6]. About one-third of severely disabled people (~4% of US population) need personal assistance for daily activities. In 2011, 5.2 million adults required help with Activities of Daily Living (ADLs) such as eating or bathing, and 9.8 million adults required help with instrumental activities of daily living such as household chores or shopping [6]. Brain injuries, such as those due to a stroke and blunt force trauma, and peripheral injuries such as those due to a spinal nerve injury, are often the most commons reasons for motor impairments in the upper and lower limbs of persons with disabilities [7]. Impairments then affect the ability of the person to exert the voluntary control over the muscles needed to do common activities such as walking or drinking from a glass. The following describes some of these target populations and their common motor impairments requiring physical rehabilitation.

A stroke (cerebrovascular accident) occurs when blood flow to the brain is significantly reduced due to ischemia or hemorrhage [8]. With less blood flow, oxygen is limited and brain cells die, which typically damages one's ability to control body movements. Strokes range from mild temporary weakness in a limited set of muscles to permanent paralysis on one side of the body. Typically, a stroke is categorized as mild, moderate or severe using the Fugl-Meyer Upper and Lower Extremity motor scale which rates per limb, a person's control over one or more joints [9]. In the United States, a stroke occurs about every 40 s [6]. About 795,000 Americans suffer a stroke each year

and approximately 600,000 of these incidents are first-time strokes, and 195,000 are recurrent attacks. About 5.8–6.5 million US adults live with the effects of a stroke [6]. Rehabilitation typically focuses on re-learning independent living, such as reaching, grasping, bathing, eating, and walking. Because a stroke can impact a very specific set of limb movements, to maximize improvement, clinicians employ mass repetition of focused movements and the application of adaptive forces to support the limb movement as needed. Clinicians often motivate patients to use their injured body segment, which may otherwise be neglected. Therefore, when designing devices, engineers should consider the importance of targeted massed repetition, motivation, and the tendency to neglect use of injured limbs.

Cerebral palsy (CP) is the leading motor disability in children, with an estimated 1 out of 323 children in the United States being diagnosed with some form of CP [6]. CP is associated with impairments in motor, cognitive, and sensory systems. CP is a motor disorder caused by brain lesions that occur prenatally or, in some cases, before the age of 2 years. According to the United Cerebral Palsy Association, it is estimated that more than 700,000 Americans have CP [10]. Characteristic symptoms of CP include spasticity, muscle weakness, rigidity, and loss of selective motor control [10]. The most commonly used classification system is based on gross motor ability. Patients with a high level of gross motor ability can walk independently and may have excessive tightness in one or more muscles (spasticity) resulting in higher energy expenditure, slower gait, and poor balance. In contrast, patients with a low level of gross motor ability spend most of their day in a wheelchair and remain heavily dependent on caregivers. Common gait patterns among children with spastic cerebral palsy include ‘crouch gait’

and ‘jump gait’ [11]. Sometimes these can be improved through surgery, but often that is not enough. Engineering technologies for patients with CP depends widely on the severity of CP and include facilitation and training of upper extremity motion, gait, and balance. The goal of management of cerebral palsy is to increase functionality, improve capabilities, and sustain health in terms of locomotion, cognitive development, social interaction, and independence.

There are 250,000 to 400,000 people in the United States with spinal cord injuries or dysfunction. About 12,000 people in the United States suffer a traumatic spinal cord injury (SCI) each year [6]. In contrast to stroke, a spinal cord injury primarily and specifically affects motor function associated with nerves below the spinal level of injury. Thus, patients with injury to lower levels of the spinal cord may have loss of sensation in lower legs but retain control of many actions, including some level of walking. On the other hand, patients with injury to upper levels of the spinal cord may have quadriplegia with impairments across legs, trunk, and arms. Biomechanic approaches to helping SCI have most often focused on improving or enabling gait. These include, but are not limited to, walkers, leg braces, and other prosthetic devices [12].

In all of these cases, riding on a horse or a device such as the MHS, can provide targeted repetition, training, and motion therapy in a motivating, enjoyable form.

Motor Control and Learning

Although it is known that hippotherapy can have benefits for many types of people, the mechanisms that elicit these benefits while riding are unknown. One application for the current study is to better understand how riding may result in benefits, such as improving balance. By simply affecting participants in one plane of motion,

Peterka et al. was able to prove that balance is a very complex measure that is achieved by visual, vestibular, and proprioceptive sensory systems [13]. It is believed that each system detects error from a reference position: visual from head orientation relative to the world, proprioceptive from leg orientation relative to support surface, and vestibular from head orientation relative to gravity [14–16]. They deduced that balance is mainly generated by feedback control mechanisms in the body actively generating torque during stance control in response to a stimulus in the frontal plane. In the current study, balance tests were performed before, and after riding in order to test how the body responds to the three-dimensional riding stimuli.

Falls are an important societal topic as well. Approximately 1 out of 4 adults over age 65 fall per year [6]. In 2014, older Americans had 29 million falls resulting in seven million injuries which together costs over $30 billion in Medicare costs [6]. Falls can lead to bone fracture, concussion, reduced mobility, fear, and even death. However, age alone is not a determinant of falls, as there is a wide range of balance abilities across older adults. Various factors lead to decreased balance control: muscle strength, sensory feedback, cognitive function, and biomechanical constraints [17]. In populations with certain pathologies, such as diabetes, vestibular impairment, Parkinson's disease, and cerebral palsy, the risk of falling is increased. Importantly, vestibular dysfunction is estimated to be in approximately 1 out of 3 adults over the age of 40 years [18]. Because vestibular cues provide the brain with information about where the body is with respect to the gravitational field, vestibular dysfunction can lead to poor balance, increased likelihood of falls, and decreased mobility [18].

The reason falls are so critical is because balance underlies most voluntary activities of daily living. For example, reaching for a cup or walking to one's car requires a person to maintain stability of their body against gravity and to maintain stability in response to internal and external perturbations. Internal perturbations include those generated by oneself when muscles are activated and when one body segment accelerates relative to another [19]. People typically learn to anticipate the effects of internal perturbations and are rarely aware of their presence. However, in certain pathologies the anticipation of internal perturbations is not fully learned. External perturbations include gravity and disturbance from the surroundings, such as an uneven surface or bumping into another person. External perturbations are often not anticipated and require appropriate reactive strategies for activating the appropriate muscles with precise force and timing. Patients with balance impairments often react to external perturbations with the wrong muscles and poorly scaled responses that can put them at a greater risk of falling [18].

Therapies for older adults who are not diagnosed with a specific condition are typically more global, centered on mobility, coordination, and strength, and consistent with the principle of "use it or lose it". In contrast, vestibular balance treatments are more focused on improving vestibular integration (and reducing symptoms of dizziness) by repositioning crystals in the vestibular apparatus, or are aimed at improving a patient's ability to make corrective torque [20]. For patients with more severe posture impairments, balance treatments may focus on the basic task of upright sitting. There is increased emphasis on the value of using a stimulus (termed perturbation training) in treatment for all populations. Unexpected perturbations require active balance responses,

and predictive perturbations help patients practice anticipatory responses [20]. Delivering repeatable and safe perturbations almost always involves biomechatronics technology, such as may be provided by riding on a horse, or on a device such as the MHS.

Finally, in addition to balance, the massed practice associated with hippotherapy could directly improve gait kinematics. It is obvious that there is an interaction between gait and balance. For example, foot placement corresponds to base of support and the body motion must be controlled to achieve balance. During gait, sagittal plane motion is heavily influenced by passive mechanics while frontal plane motion is heavily influenced by sensory feedback [21]. Hippotherapy evokes pelvis motion similar to gait and therefore has the potential to train synergistic activities to improve gait.

Therapeutic Uses of Horses

For thousands of years, the horse has been a companion and aid to mankind. From a form of transportation to a means of entertainment, horses have been utilized for a variety of reasons [22]. As times have changed, so have the uses for horses. In approximately the 19th century, a more recent use, known as hippotherapy, was discovered [4]. Hippotherapy, which is the use of therapeutic horseback riding in order to increase coordination, strength, and balance, has shown to have a positive effect on motor control and overall well-being for children with disabilities such as cerebral palsy (CP) [3,23,24]. It has also been suggested that hippotherapy can improve gait speed and reduce psychological symptoms in patients with multiple sclerosis (MS) [25]. In addition to neurological disabilities, hippotherapy can be used to improve balance and gait symmetry in stroke patients [1,26] Cho et.al also showed that hippotherapy has the

ability to increase levels of cortisol and serotonin in elderly riders after a 8 week riding period [27]. It can be inferred that these beneficial hormones would also increase in disabled riders as well. As mentioned above, hippotherapy provides unexpected perturbations to the rider, requiring them to actively respond and predict upcoming perturbations.

Although the benefits are well documented, hippotherapy is not without limitations. Many people who suffer from these disabilities, or the clinics that treat them, may not have the funds or space to accommodate a live horse. Therapy horses must undergo extensive training in order to be used with disabled patients. In addition to having a gait pattern that is sufficient for therapy, the horse must be very calm and gentle with the riders [4]. Ability to ride a horse can be weather-dependent if the riding facility is not indoors. Furthermore, some patients may have allergies or fears about being around or seated on top of such large animals. Allergens such as dust, hay, and animal dander are also quite common in stables or arenas. It was with these limitations in mind that the idea for the MHS was conceived, to provide a complimentary tool that provides the complex riding motion in a safe, convenient way.

For many years, physical therapists have aimed to increase motor control and stability through exercises that require the patient to actively produce a given the movement. However, there has been increasing interest in the use of complex, unpredictable motion patterns that impart a motion to the patient. It has been proven that these motions can develop and reinforce neural and motor pathways by challenging balance and coordination [2]. These exercises can stimulate muscles that otherwise would not be accessed by ordinary physical therapy methods. A common method for

imparting motion to the patient is through the use of an exercise ball. The patient balances on the ball while the therapist moves the ball around. However, the range of motion and the motion pattern of the ball are limited, and the pattern may vary a lot between therapists or between sessions. Another method is the use of weight-supported treadmill training, which takes some load off the patient while they exercise on a treadmill [28]. This seems to be an effective method to help the patient regain muscle control, but it has been proven that walking on a treadmill elicits a different response than walking on flat ground [29,30].

The mechanical horse-riding simulator (MHS) was designed and developed at Baylor University by Dr. Brian Garner to address all of these reasons. It is intended to provide a safe, convenient, complimentary tool for therapy with the comlex, three-dimensional motion pattern of horse riding. Derived from the motion of a real horse, the MHS imparts a motion to the rider, who sits about standard table-height on the cushioned, hemispherically-shaped seat. The seat motion is powered by a single electric motor that runs a series of pulleys and levers with speed variability from a very slow walk to a brisk walk. The setting used in this study runs at a speed of 36 complete riding motion cycles per minute. The MHS can be seen in Figure 1. Figure 2 shows angular motions for one full cycle of the MHS and one full walking cycle of the target motion from a real horse. The MHS motion is shown by the dotted line while the real horse motion is represented by the solid line in the frontal (roll), sagittal (pitch), and transverse (yaw) planes. The MHS cycles are clearly very similar to real horse target motion.

Figure 1: The Mechanical Horse-Riding Simulator (MHS). The MHS is a stationary device with a saddle seat structure that moves with the complex, three-dimensional motion pattern generated by a horse under normal walking gait. It was inspired by equine assisted therapies (e.g., hippotherpy) as a complimentary tool to make such therapies more broadly and conveniently accessible.

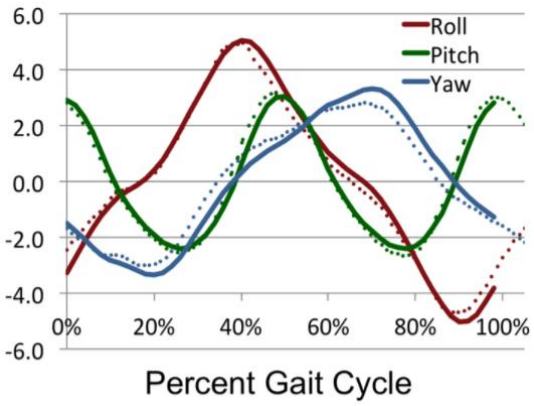

Figure 2: Horse Vs. MHS Motion Cycle in Degrees. Horse motion is represented by the solid line while MHS is represented by the dotted line.

Although there are other mechanical horse simulators on the market, none is designed like the MHS. For example, the "Always a Good Ride" riding simulator is shown in Figure 3 [31].

Figure 3: Always A Good Ride Simulator

This simulator, while impressive, is geared more towards those who want to race horses or jump obstacles. It is similar in looks to a real horse and can imitate different types of competitions such as dressage, show jumping, and cross country riding. It is also extremely expensive for the unit and requires a computer monitor for the riding simulation video.

Another simulator is called the “Equicizer” (Figure 4), which was originally designed to train people who want to race horses competitively [32].

Figure 4: Equicizer Horse Simulator

Although no motion data has been published for these simulators, video sequences reveal that they both move in the singular, sagittal plane (forward/backward and up/down.

In addition to these two, there are a number of other riding simulators such as the RaceWood equestrian simulators, the iGallop, and the Panasonic Joba. The RaceWood simulators are similar to the "Always a Good Ride" in that it is very expensive and is designed for equestrian gaits, not therapeutic motions. The iGallop and Panasonic Joba impart motion to a rider designed to jiggle the core of healthy riders for building core muscle strength. The Panasonic Joba has shown ability to significantly improve static and dynamic balance in children with cerebral palsy [1].

Gait Training

One of the main goals therapists have for rehabilitation of children with cerebral palsy is teaching them how to improve their gait patterns to make it easier and more efficient for them. Riding on a horse has been shown to exhibit movement patterns quite similar to those of healthy human walking in children [5]. For example, Garner et al. showed that displacement amplitudes and pelvis motion trajectories were very similar between riding the live horses and walking for the children. They were also able to show that riding motions between different horses varied more than the motion patterns between walking and riding. These similarities suggest the possibility of horse riding being able to rehabilitate a disabled child's walking motion by imparting a normal gait motion to them. Another recent case study involving a child with cerebral palsy found that a 12 week session of mechanical hippotherapy significantly decreased the normalized sway area of the stance phase during walking [33]. In addition, the size of the transverse abdominal and lumbar multifidus (two important postural muscles) significantly increased. It is reported that the average walking speed for an able-bodied population is about 1.40 m/s , but is much slower in people with disabilities such as

stroke (about .4 m/s) [34]. Nymark et al. concluded that, as one might expect, in a nondisabled population the EMG activations in lower limb muscles and the lower limb range of motion was less at slower gait speeds than at normal speeds. Thus people with gait-limiting disabilities may not be generating as much muscle force as the non-disabled, leading to more muscle atrophy and gait inefficiencies. In this study EMG data are collected during riding to evaluate the extent to which gait-related muscles are activated.

Current Treatment Technology

The concept behind the MHS is consistent with the general trend to leveraging technology in rehabilitation. For balance training, some of the most common technologies include Wii sports in clinics (which includes biofeedback of arm movements or forces generated under the feet) and wearable sensors such as FitBits that can detect general activity levels. Many of these approaches are used in patients with specifics conditions, such as SCI, Parkinson's Disease, and stroke [6]. Similarly, for children with disabilities such as mild-to-moderate CP, balance training may include perturbation training and the inclusion of video games [35]. Video games can increase motivation and offer the potential for greater specificity of training and feedback. For those with milder impairments, off the shelf systems such as Wii and Kinect have been used to increase muscle strength and coordination and endurance [35]. For those with more severe CP, typically customized engineering is required.

When perturbations are included in devices, they typically include an external force (push or pull), surface motion (moving platform or sudden change in acceleration on treadmill), or a moving visual stimulus. Any system that requires balance responses can be considered perturbation training. Some examples include the Lokomat and other

lower extremity exoskeletons. These use robotic technologies attached to the patient to recreate and eventually reteach them a desired gait pattern. However, it is noteworthy that for children with CP, hippotherapy and simulated hippotherapy have provided some of the strongest evidence for improvement in areas outside of just balance [36]. Hippotherapy, along with the use of adaptive seating, was found to also improve sitting posture and postural control. In mechanical horses, these improvements may be attributed to 1) the similarity in pelvis motion between human gait and riding a horse, and 2) the high number of balance corrections practiced during a typical riding session [5].

Finally, while balance therapy is typically associated with standing or walking, the basic skill of independent sitting with respect to gravity is not something everyone can accomplish. People with neurological disorders or severe spinal cord injury may have an inability to sit independently or control one's head against gravity. For these individuals, fewer treatments are available, and these treatments require different technologies. For children with impaired trunk and head control, research has demonstrated improvement in function when seating devices are implemented [36]. Mechanical engineering is involved in creating seating systems that are comfortable and biomechanically effective. For populations with severe balance impairments, it may be necessary to combine mechanical trunk support with robotic technologies.

CHAPTER TWO

Methods

The objective of the current study was to evaluate the kinematic effects and muscular activations while riding the mechanical horse simulator (MHS) and the immediate effects it had on balance in a healthy population. All testing was done at the Baylor BioMotion lab in the Baylor Research and Innovation Collaborative in Waco, Texas. The lab, which can be seen in Figure 5, includes 3D motion capture, force plates, and EMG. One researcher performed all studies with an assistant to run the computer during collections. The same researcher placed all motion capture markers and EMG electrodes on the participants and gave instructions throughout data collections. The motion capture in the lab consists of 14 Vicon Vantage Cameras (Vicon Motion Systems, LTD, Oxford, UK). There were also three force plates for walking and balance data (Advanced Mechanical Testing, Inc, Watertown, MA) and eight electrodes for muscle data collecting at 1500 Hz (EMGs, Noraxon, Scottsdale, AZ). This section will explain each activity performed by the participants as well as the markers that were placed on them.

Figure 5: Baylor Biomotion Lab

Participants

The study was approved by the Baylor Internal Review Board, and written consent was obtained from all eleven healthy participants (8 males, 3 females). All participants were in good health with no disabilities, and ranged in age from 11 to 41 years (average was 22.7 ± 9.3 years). In order to minimize motion capture marker movement and optimize EMG reading, the participants were required to have a normal BMI (< 25) [37]. The participant body masses ranged from 46.4 to 91.3 kg (average was 71.6 ± 17.4 kg). Three of the participants had previous ridden the MHS and only one had extensive experience riding a real horse.

Motion Capture

In order to analyze kinematics of human motion in activities such as gait, motion capture systems are used by bio-mechanists. First appearing around the 1970's, motion capture technology is now starting to become widespread [38]. There are various types of motion capture systems ranging in price from hundreds of dollars up to hundreds of thousands. To better understand motion patterns, markers are placed on bony landmarks across the participant's body and tracked in three dimensional spaces by cameras set up

around the participant. By triangulating three-dimensional locations of these markers, body segment kinematics are estimated by the system software. Motion capture has been used to study individuals with disabilities. For example, a study conducted by Klotz et al. determined from motion capture that the largest reduction in range of motion between an able bodied group and a group with hemiplegic cerebral palsy was in the supination and pronation of the elbow [39]. That study also reported statistically significant differences between the lateral sway of the trunk and flexion/extension of the shoulder. Motion capture data was collected in the current study at 120 Hz in order to analyze the trunk kinematics of the rider in comparison to the motion of the MHS.

Motion Capture Marker Placement

Before the first collection, four motion capture markers were placed on the corners of the MHS seat structure in order to collect kinematic data on the imparted motion. Once the participant had signed the consent form (see Appendix D), a total of 39 markers were placed on them according to the Plugin Gait setup given by the Vicon Nexus system [40]. The marker placement used in this study can be seen in Figure 6. This minimalist marker setup reduces time of placement and overall collections as well as focuses on the key markers needed for this study (trunk). Because it is a passive marker system, people of all body sizes are able to be used for the study. Other benefits include eliminating the need for a power source required by active motion capture systems and maximizing range of motion for the participant. Markers generally were placed near bony landmarks on the body in order to reduce inaccuracies due to bouncing skin. Key markers that will be referenced later are the LPSI, RPSI, C7, LSHO, and RSHO.

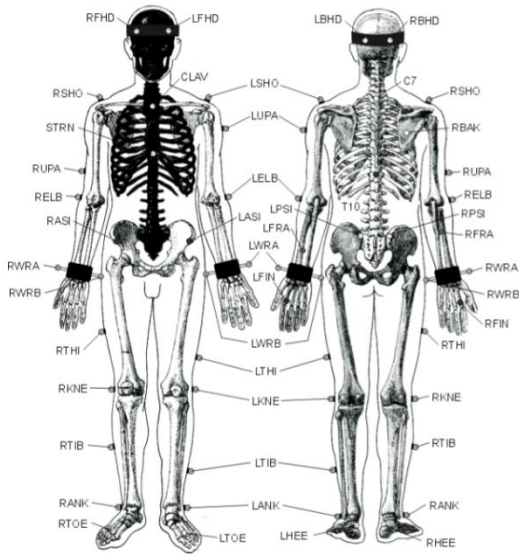

Figure 6: Plugin Gait Marker Placement

Electromyography

Electromyography, also known as EMG, is a recording device that measures the electrical potential of muscle tissues as they undergo stimulation. Every time a muscle is contracted, voluntarily or involuntarily, a voltage is sent through the muscle, which is then recorded and represented by the EMG system graphically, numerically, or by sounds [41]. The signals are used to detect medical abnormalities, activation levels, recruitment order, or analyze biomechanics [41]. EMG uses surface or needle electrodes to record voltage potential data from the muscles. Needle electrodes generally are used to collect more accurate data, especially in deep muscles, but can be a little painful for the participant. Therefore, it is much harder to recruit test participants for needle electrode studies. Surface electrodes, on the other hand, are limited to only superficial muscles and make it hard to collect data on overweight participants due to extra subcutaneous fat between the skin and muscle that interferes with the signal. Before the surface electrodes are placed, the skin must be wiped with an alcohol pad to clean off dirt or excess oils and

sometimes shaved for hairy participants. This study used surface electrodes for all data collections.

Although it can be hard to perfectly place the electrodes on the desired muscle with either type of electrode as there is no exact science to it, EMG can be used for a variety of reasons. These include, but are not limited to, diagnosing muscle or nerve dysfunction, identifying which activities stimulate certain muscles, and measuring maximal voluntary contraction. Using EMG is a very low risk procedure with the only risk being if an unclean needle electrode is used, possibly causing infection. Fatigue of a muscle can also be measured with EMG by an increase in the mean absolute value of the signal, increase in the amplitude and duration of the muscle action potential, and a shift to lower frequencies [42]. When used with motion capture, EMG can help evaluate muscle control in relation to CoP changes from external perturbations for the purpose of studying balance measurements [43].

EMG Electrode Placement

In the current study, manual manipulations were performed to locate 4 different muscle groups bilaterally: upper abdominal, gluteus maximus, lumbar, and hamstring. These muscles were chosen because they are key stabilizer muscles used during walking and riding (except the hamstrings during riding). The skin covering each of these muscles was rubbed with alcohol wipes to remove any excess dirt and oils. The skin was then dried, and Noraxon EMG dual electrodes were placed as near to the center of the muscle head as possible as to maximize signal readings. The signal transmitters were then clipped onto the electrode and attached to the skin nearby using an adhesive (off the muscle that the sensor was placed on) as a ground where the participant's motion would

not cause them to fall off. The placements were taken from the Noraxon 3.8 electromyography software and can be seen as the highlighted dots in Figure 6 [44].

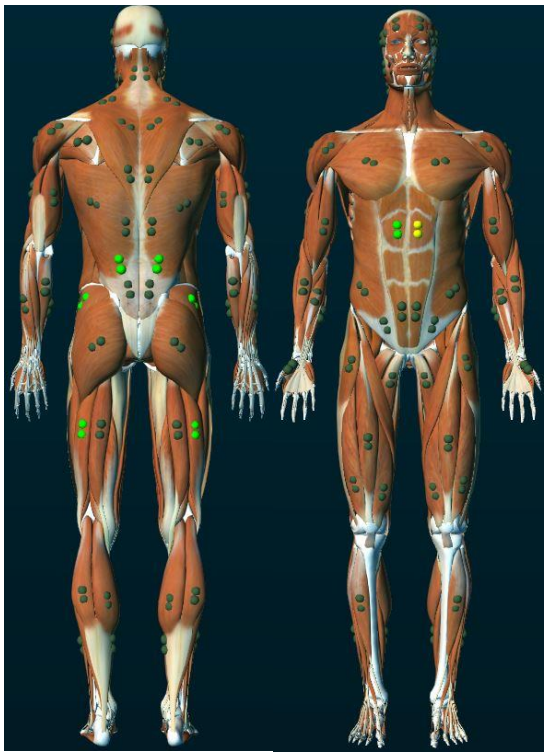

Figure 7: EMG Electrode Placements

Pre-Ride Protocol

In order to normalize the EMG data, three maximum voluntary isometric contractions (MVIC) were performed for each of the muscle groups during five second tests. These were taken from a number of previous studies that normalized EMG data [45–47]. To test the abdominals, the participant was strapped into a Biodex dynamometer in a seated position with feet off the ground and hands at their side and told to sit up as hard as possible for five seconds. To test the hamstrings, the participant lay prone on a massage table and tried to pull their foot up by only bending the knee while the researcher held their foot in place at a 90° angle for five seconds. The lower back

muscles (lumbar) and glutes were tested by laying prone with the hips on the edge of the massage table and legs hanging off. The participant then straightened and lifted the legs, contracting the back as hard as possible. A series of exercises to test balance and flexibility were then performed including the following. The first was laying prone on a medical table with knees on the edge and extending the straight legs as far back at the hip as possible while alternating legs for three repetitions on each side. This can be seen below in Figure 8 [48].

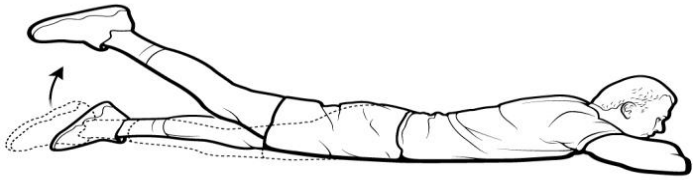

Figure 8: Alternating Hip Extension

The second exercise was standing upright on one AMTI force plate and touching the toes three times (or as far down as possible) while keeping the legs straight. The first two balance tests consisted of one-legged (left and right) balancing with eyes open for 15 seconds standing on the force plate. The third balance test consisted of standing on the force plate with both feet together and eyes closed for 60 seconds. The final exercise was a normal walking trial across the lab (approximately 20 feet) across all three force plates.

Riding Protocol

The participants rode on the MHS while keeping their back straight and upright with the head facing forward for five minutes at a speed corresponding to 36 gait cycles

per minute, which corresponds to a modest walking gait speed on a horse. Figure 9 shows one of the riding participants. Data was collected for the first 30 seconds, the middle 30 seconds, and the last 30 seconds of the ride.

Figure 9: Proper MHS Riding Form

Post-Riding Protocol

After completing the 5 minute ride, the participant immediately got off the MHS and repeated the same exercises performed before riding (excluding the MVIC trials), beginning with the eyes closed, two-legged balance test. A 5 minute break was then taken where the participant was offered water and sat down to relax. After the break, the participants repeated the exercises for a third time. Finally, the markers and electrodes were removed from the participant and cleaned with alcohol wipes for future collections.

CHAPTER THREE

Results

Pre/Post Ride Balance Measures

As explained in Chapter Two, three rounds of the balance tests were performed: one pre-ride, one immediately post-ride, and one approximately five minutes after the first post-ride. From the three balance tests with feet together eyes closed (FTEC), three measures were drawn: center of pressure in the x direction (CoPx), center of pressure in the y direction (CoPy), and moment about the z axis (Mz). In this study, the x direction is forward/backward for the participant (anterior/posterior), the y direction is side to side (mediolateral), and the z is up and down (superior/inferior). In figure 10, a sample of the CoPx, CoPy, and Mz vs time as well as the CoPy vs CoPx, can be seen for the entirety of the three FTEC balance tests of participant 1. For clarity in the Mz graph, the pre-ride is shifted up 200 units (Nm) while the post-ride 2 is shifted down 200 units. Likewise, in the CoPy vs CoPx graph, the pre-ride measures are shifted 20 units (mm) to the left and up while the post-ride2 measures are shifted 20 units to the right and down in order to visualize the shapes of each graph. It can be seen that throughout the three tests, there were no drastic changes in this healthy participant, as to be expected. A collection of all three balance tests analyses (two feet with eyes closed, left leg with eyes open, and right leg with eyes open) can be found in Appendix D for each individual participant.

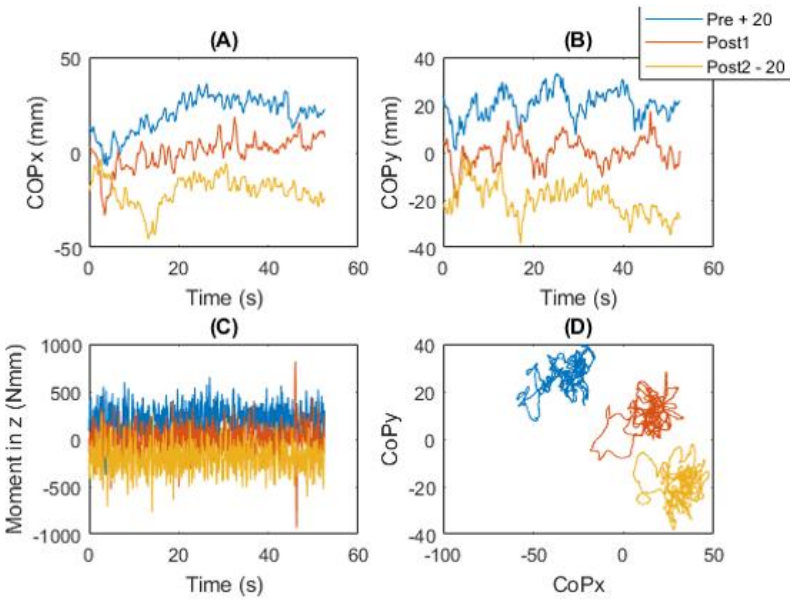

Figure 10: Balance Test Measures over Entire 60 seconds for Participant 1. Blue lines indicate the pre-ride test, red indicate the first post-ride, and yellow indicates the second post-ride (A) is the CoP in the x direction. (B) is the CoP in the y direction. (C) is the moment about the z direction. (D) is the CoPy vs CoPx.

Figure 11 shows the standard deviations in all three planes (CoPx, CoPy, and Mz) of participant 1. The blue bar represents the pre-ride, the red bar represents the first post ride, and the yellow bar represents the second post-ride.

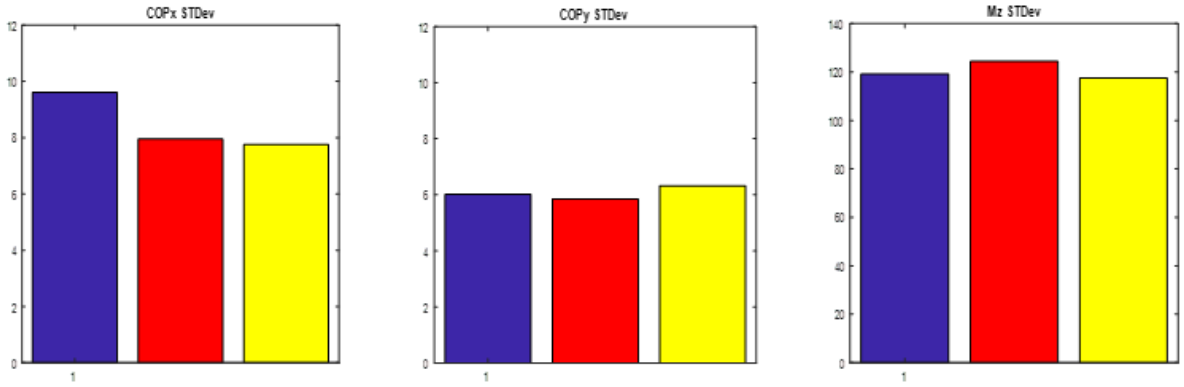

Figure 11: Standard Deviations of Balance Tests for Participant 1. The blue bar represents the pre-ride balance standard deviation, red bar represents the post-ride 1, and yellow bar represents the post-ride2. The first chart is the CoP in the x direction. The second chart is the CoP in the y direction. The third chart is the moment about the z direction.

Like previous balance studies, the root mean square (RMS) of all participants' balance data was computed [49,50]. The Matlab code for this particular calculation can be found in the beginning of Appendix A. This was done in accordance to similar methods used in a previous balance study that evaluated responses to perturbations in one plane [49]. Figure 12 shows the average RMS among all eleven participants for each test. Again, each bar represents one test (Pre, Post1, and Post2). Note that the trends are very similar among one participant and all participants averaged together.

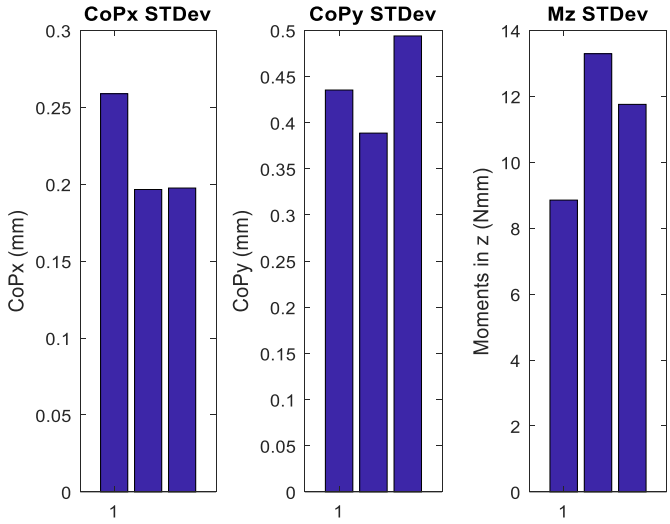

Figure 12: RMS of Two Footed Eyes Closed Balance Measures From All Participants. (A) is CoPx, (B) is CoPy, and (C) is Mz. The first column of each graph represents the pre-ride test, the second column represents the first post-ride test, and the third column represents the second and final post-ride test.

The average standard deviations in the figure above can be seen in Table 1 for easier numeric comparisons. It should be noted that both the CoPx and CoPy measures decreased immediately after riding, while the moment measures increased dramatically after riding. Also, the moments in the z are, on average, much larger and more variable.

Table 1: Standard Deviations Across Balance Tests

Balance Test	CoPx RMS	CoPy RMS	Moments about Z-axis RMS
Pre-Ride	.2588	.4354	8.8516
Post-Ride1	.1965	.3887	13.2907
Post-Ride2	.1975	.4939	11.7551

P-values were then calculated in Matlab using the 'anova1' function in order to test for statistical significance between tests. The p-values are deemed "statistically significant" at a 95% confidence level if they are below .05. These p-values can be seen below in Table 2. None of the p-values returned statistical significance, but trends can be seen. Pre vs Post1 and Post2 are both much lower than Post1 vs Post2 in both the CoPx and Mz p-values. However, the opposite is true for the CoPy values.

Table 2: P Values for Balance Test Measures

Balance Tests	CoPx p-values	CoPy p-values	Mz p-values
Pre vs Post1	.266	.717	.1577
Pre vs Post2	.2613	.6642	.2167
Post1 vs Post2	.9806	.258	.6244

Rider Motion Compared to MHS

In order to process the motion capture data that was collected while riding, the xyz coordinates of each marker were imported into Matlab. The trunk segment was then defined as the line between the midpoint of the two PSI markers and the C7 marker. Then the angles in the frontal (roll) and sagittal (pitch) planes were calculated throughout the

ride. These were calculated as the arc tangent of the horizontal displacement of C7 with respect to the midpoint of the PSIS markers divided by the trunk distance between C7 and the midpoint [49]. For the transverse (yaw) plane, the midpoint was found between the shoulders, and the angle between one shoulder and the midpoint in the transverse plane was calculated as the arctangent of the displacement of the shoulder in the x direction divided by the distance between the midpoint and shoulder. Similarly, the angles between the PSI markers were also calculated for transverse motion of the hips. Markers were placed on the MHS as described in Chapter Two and angles of the roll, pitch and, yaw were calculated in a similar fashion in the frontal, sagittal, and transverse planes (respectively) for the MHS during the ride. Each complete cycle of the MHS was found to require duration of about 1.71 seconds at the fixed speed setting. Each thirty second trial was then cut into cycles and the average motion patterns over these cycles of both MHS and rider were calculated. These angles are shown in Figure 13 for one participant over a 30 second trial. A spatial view of the motion patterns in two planes at a time was then plotted for both the MHS and the rider. The first three combinations (frontal vs sagittal, frontal vs transverse, and sagittal vs transverse) can be seen in Figure 14 for participant 11 during one representative thirty second trial. The patterns between the horse and the rider are strikingly similar, with a slight delay between the two. Also, it should be noted that the highest range of amplitudes occurs in the sagittal plane.

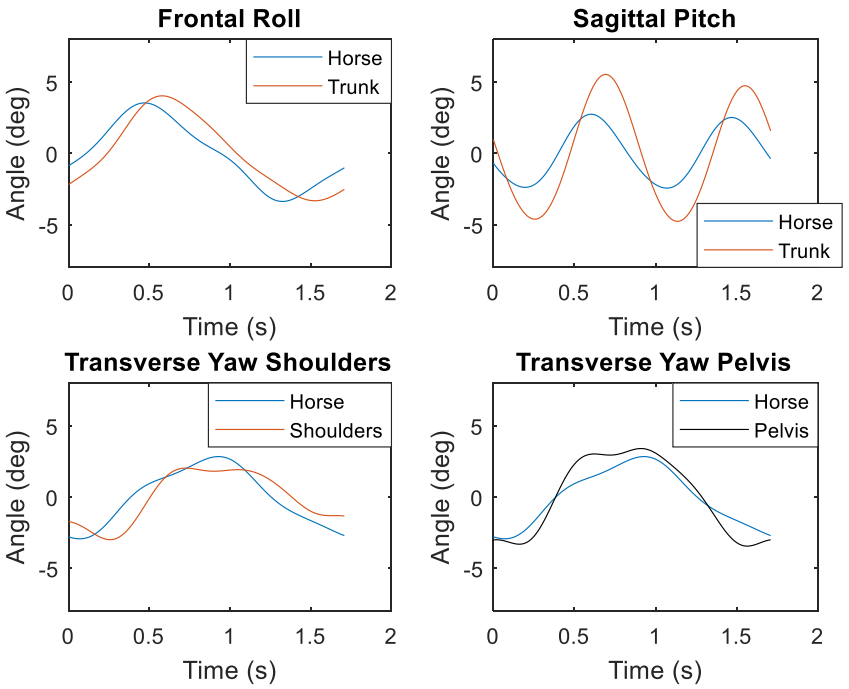

Figure 13: MHS and Rider Kinematic Angles vs Time. Top left is the Frontal Roll of Horse and Trunk. Top right is the Sagittal Pitch of Horse and Trunk. Bottom left is the Transverse Yaw of Horse and Shoulders. Bottom right is the Transverse Yaw of Horse and Pelvis.

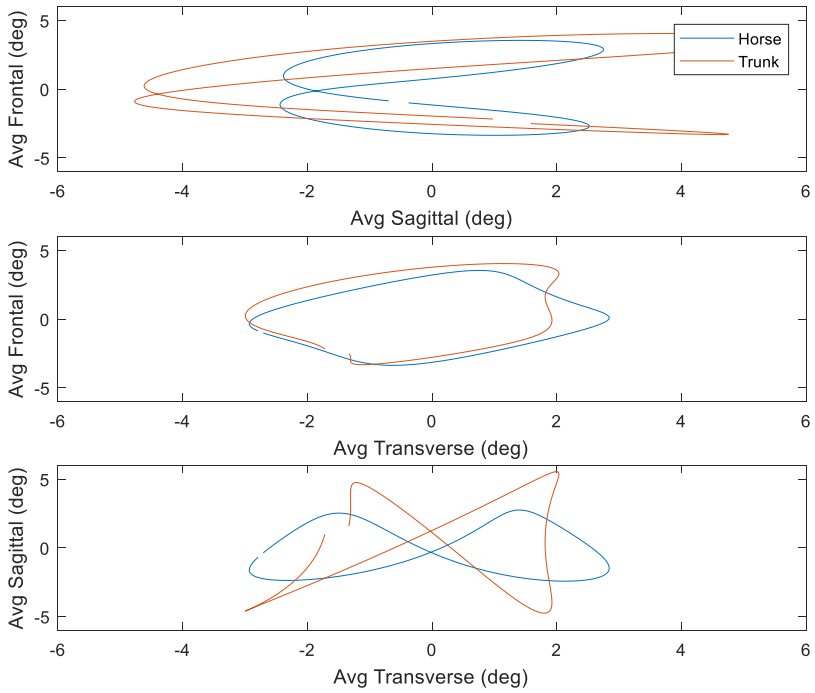

Figure 14: Angle Vs Angle Plots of Horse and Rider During One Average Motion Cycle of One Participant

Average Motion Across All Riders

In each plane, all 11 riders' trunk motions were averaged together across each of the three 30 second collections (beginning, middle, and end of the five minute ride). Also the standard deviation of each rider was found over cycles and averaged together, which are shown as thin black lines above and below the mean angle in blue in the following figures. Angles in the frontal plane for the average cycle can be seen in Figure 15. The top graph is the beginning 30 seconds, the middle is the middle 30 seconds, and the bottom is the final 30 seconds of the five minute ride. Angles of the trunk in the sagittal plane can be seen in Figure 16. The angles of the shoulders in the transverse plane can be seen in Figure 17. The angles of the pelvis in the transverse plane were also calculated and are found in Figure 18. These motion patterns stayed very consistent between all riders with relatively low standard deviations. Figure 19 shows the four previously mentioned graphs without standard deviations, and with the three 30 second recording windows together. The three riding trials for each plane were combined and put into this one graph to more easily assess the changes throughout the five minute ride. Over the five minute ride, the average motion cycle is very similar, but it does seem as though the middle thirty seconds is a little bit ahead of the other two trials. The range of means and standard deviations of each trial in all three planes can be seen in Figure 20.

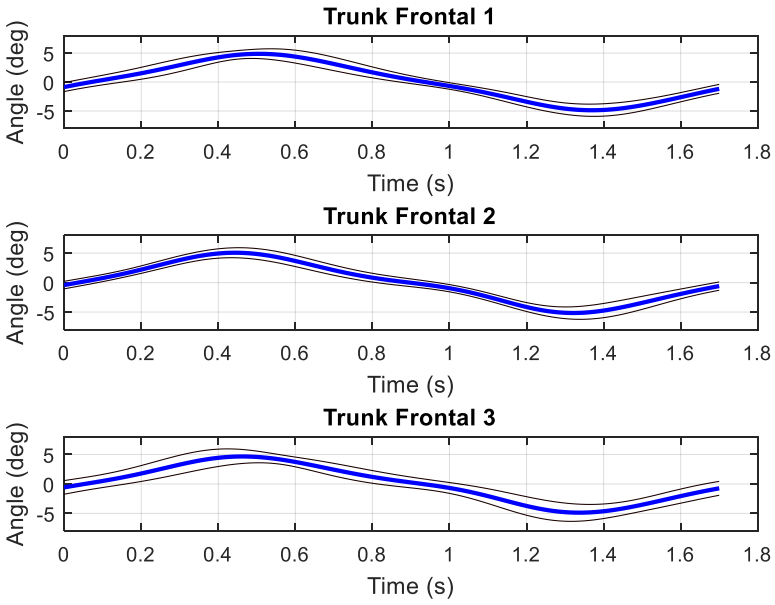

Figure 15: Average Frontal Plane Motion of One Horse Cycle with standard deviations. (A) is the first 30 seconds of ride. (B) is the middle 30 seconds of ride. (C) is the final 30 seconds of ride.

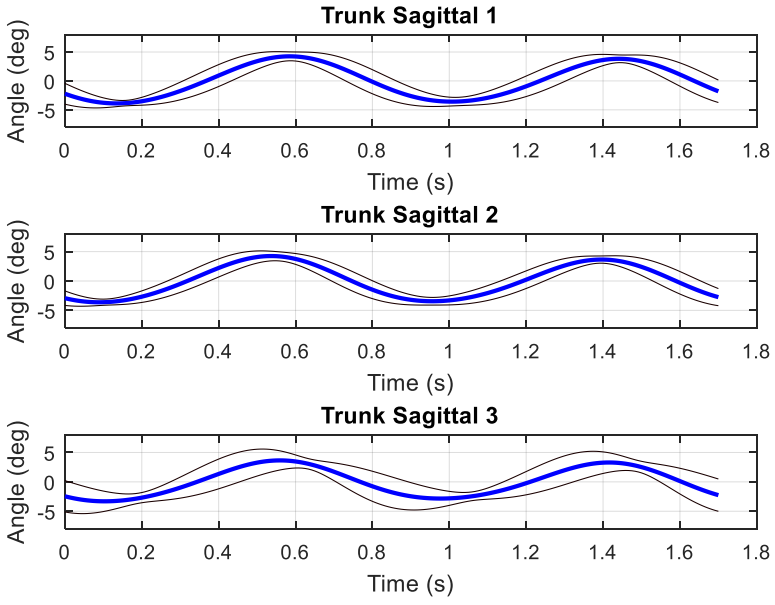

Figure 16: Average Sagittal Plane Motion of One Horse Cycle with standard deviations. (A) is the first 30 seconds of ride. (B) is the middle 30 seconds of ride. (C) is the final 30 seconds of ride.

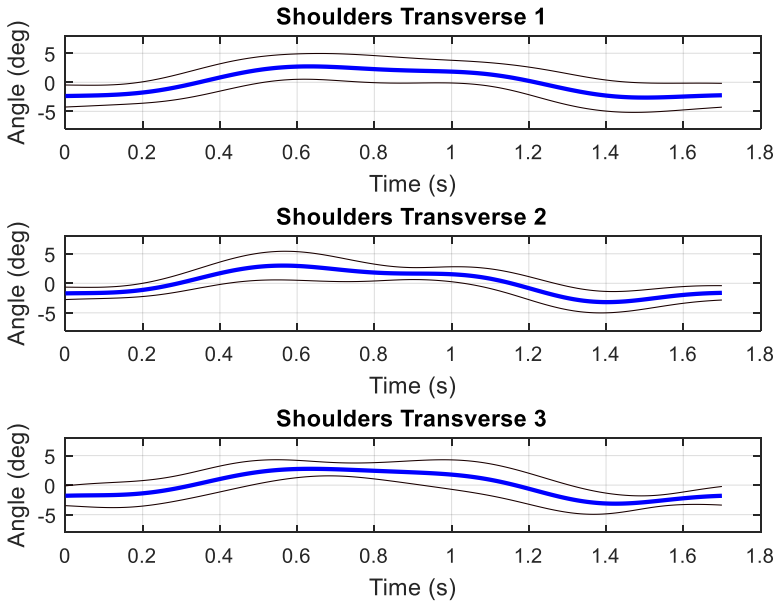

Figure 17: Average Shoulder Transverse Plane Motion of One Horse Cycle with standard deviations. (A) is the first 30 seconds of ride. (B) is the middle 30 seconds of ride. (C) is the final 30 seconds of ride.

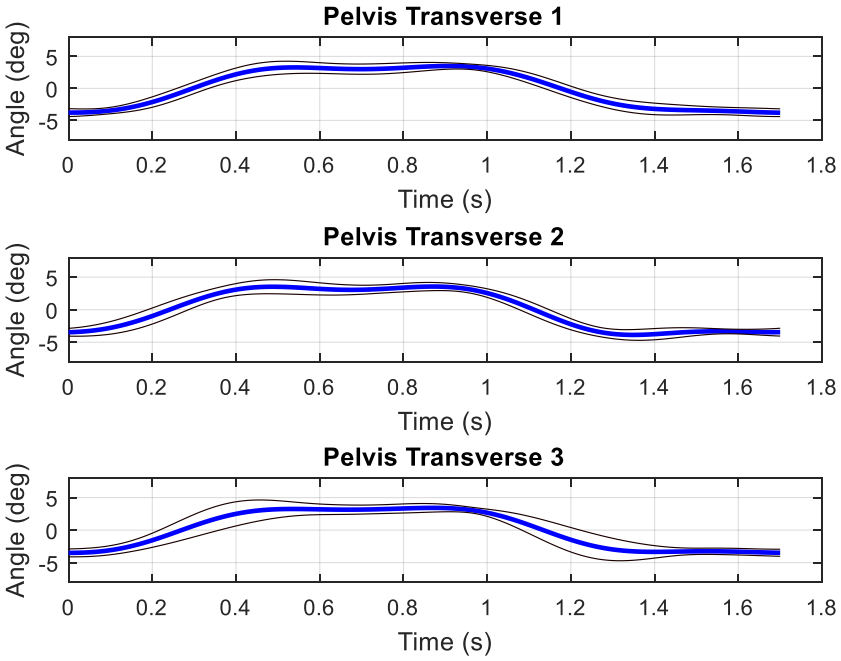

Figure 18: Average Pelvis Transverse Motion of One Horse Cycle with standard deviations. (A) is the first 30 seconds of ride. (B) is the middle 30 seconds of ride. (C) is the final 30 seconds of ride.

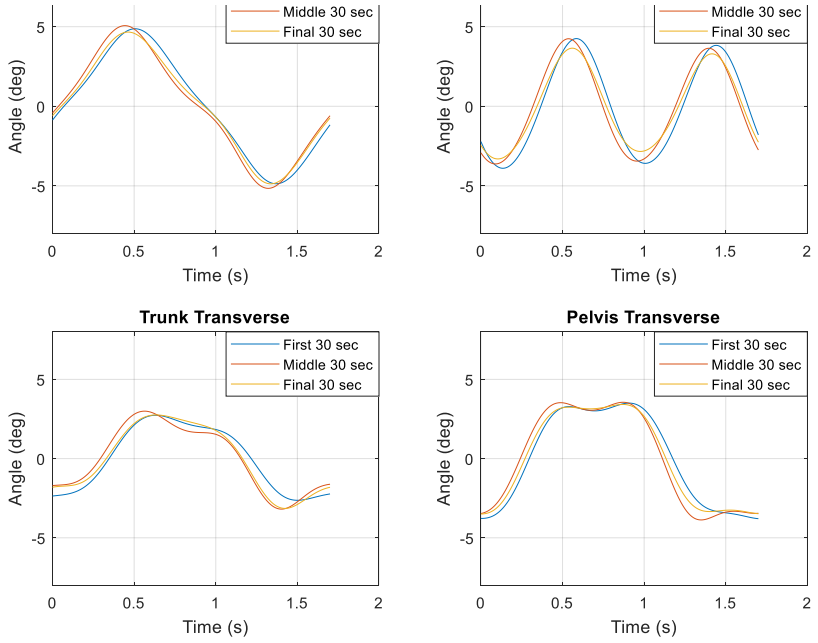

Figure 19: Average Motion of all Planes and all rides. (A) is trunk motion in the frontal plane. (B) is trunk motion in the sagittal plane. (C) is the shoulder motion in the transverse plane. (D) is the pelvis motion in the transverse plane.

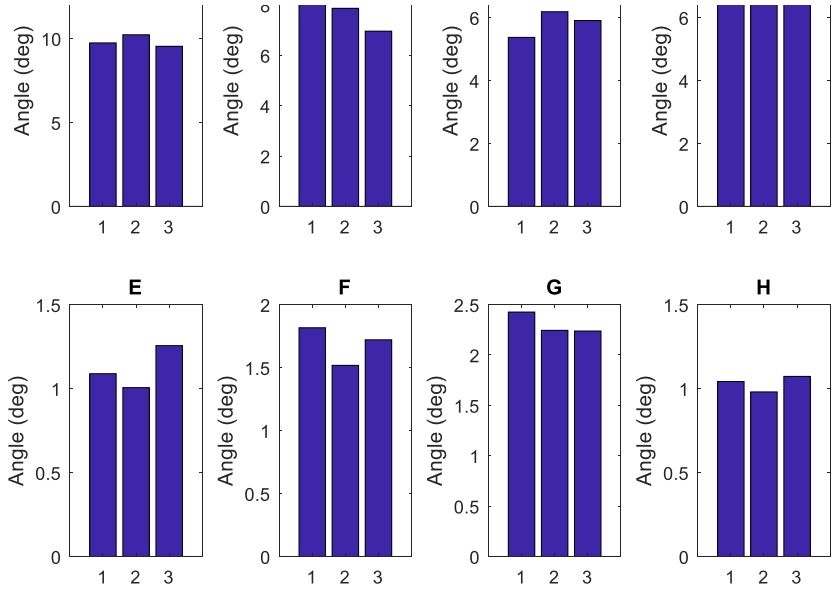

Figure 20: Range of Means and Average Standard Deviations of Trunk Motion. 1 is the first 30 seconds, 2 is the middle 30 seconds, and 3 is the final 30 seconds. (A) and (B) are trunk ranges in the frontal and sagittal plane, respectively. (C) is the shoulder range in the transverse plane. (D) is the pelvis range in the transverse plane. (E-H) are the corresponding standard deviations.

The coefficients of variation (CoV), which are calculated as the standard deviation divided by the mean, across the three collections, can be found in Table 3. Only the transverse motion of the shoulders is shown in this table, in the third column. From Table 3, one can take away that the CoV drops after the first thirty seconds and increases again before the end of the five minutes in all three planes. The CoV were largest in the transverse plane at an average of .398 (sagittal average of .221 and frontal average of .114). Fittingly, the standard deviations in the transverse plane were also by far the largest averaging 2.303° as opposed to 1.685° in the sagittal plane and 1.117° in the frontal, meaning each participant varied the most in the transverse plane while riding. In the frontal and sagittal planes, the standard deviation decreased in the middle of the ride and increased again towards the final thirty seconds.

Table 3: Coefficients of Variation across Five Minute Ride

Trial Number	Frontal Plane	Sagittal Plane	Transverse Plane (shoulders)
1st Trial (First 30 sec)	.1118	.2229	.4519
2nd Trial (Middle 30 sec)	.0984	.1929	.3629
3rd Trial (Final 30 sec)	.1318	.2474	.3793

To show how similar the motions were, the correlation between the MHS and each rider was calculated by using the "xcorr" function in Matlab and finding the maximum correlation between the two functions (MHS and trunk angle). The correlation in all three planes for each trial was then averaged across all riders, and the results are

shown in Table 4. For the transverse plane, only the motion of the shoulder was used because it more accurately represented the yaw of the trunk. The closer the number is to one, the closer the trunk is to the motion pattern of the MHS. It should be noted that the correlations are much smaller in the transverse plane than the other two planes. This is in agreeance with Table 3, which showed that the transverse motion varied the most over the course of the rides.

Table 4: Average Correlations Between Horse and Trunk Motion

Riding Trial	Frontal Plane	Sagittal Plane	Transverse Plane (shoulders)
1st Trial	.9896	.9772	.8679
2nd Trial	.9941	.9701	.8298
3rd Trial	.991	.9684	.8401

Another way of looking at this data is to evaluate it in the frequency domain. This approach provides more detail into the kinematic responses of the rider to the horse by decomposing the motions into specific frequencies. The amplitude spectra were calculated as the magnitude of the discrete Fourier transform for both the MHS motion and body segment motions. In Figures 21-23, the trunk and MHS motion of the three trials can be seen in the frequency domain. Figure 21 is the first 30 seconds, Figure 22 is the middle 30 seconds, and Figure 23 is the final 30 seconds. The first row of the figure is the trunk motion in each plane where the y axis is the average degree amplitude and the x axis is the frequency (in Hz). The second row is the MHS motion at each frequency, with the same axis labels as row one. Then in the third row, gain is shown for each plane, which was calculated by dividing the trunk motion by the MHS motion angles, where the

x axis is again the frequency. A gain of one indicates that the trunk tilt/rotation was equal in magnitude to the MHS at that frequency, whereas a gain of zero indicates the trunk did not respond at all to the MHS motion at that frequency. The final row is the phase lag between the horse and rider, with the x axis being the frequency and the y axis being the degree of lag. A phase of zero indicates the trunk moved with no delay in response to the MHS, whereas a negative phase indicates the rider lagged behind the MHS motion.

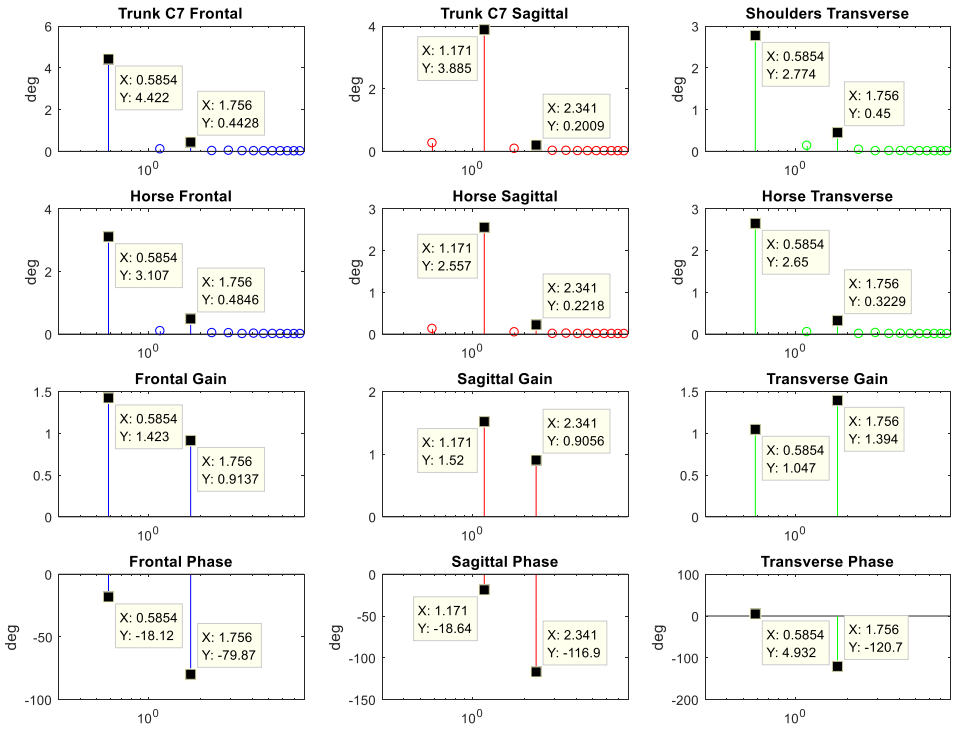

Figure 21: Frequency Domain of First Ride Trial. First row is trunk motion, second row is horse motion, third row is gain, and fourth row is phase lag. First column is frontal plane, second column is sagittal plane, and third column is transverse plane.

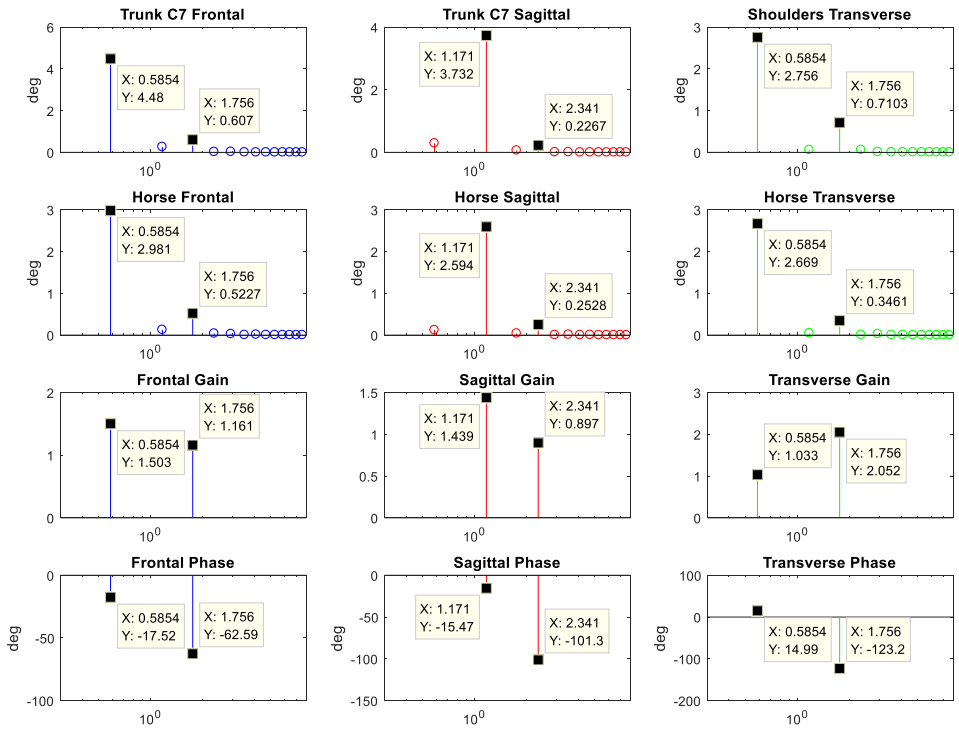

Figure 22: Frequency Domain of Second Ride Trial. First row is trunk motion, second row is horse motion, third row is gain, and fourth row is phase lag. First column is frontal plane, second column is sagittal plane, and third column is transverse plane.

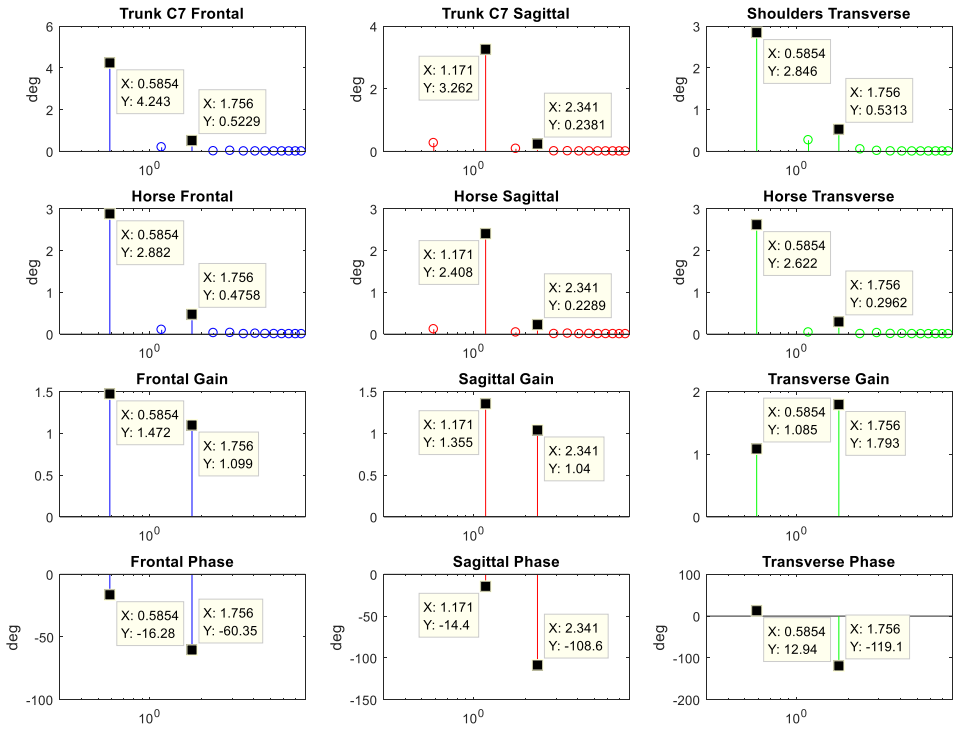

Figure 23: Frequency Domain of Final Ride Trial. First row is trunk motion, second row is horse motion, third row is gain, and fourth row is phase lag. First column is frontal plane, second column is sagittal plane, and third column is transverse plane.

The amplitude of MHS motion occurred at distinct frequencies for each of the three planes. In the sagittal plane, the MHS tilt occurred at approximately 1.17 Hz and 2.34 Hz. In the frontal and transverse planes, the MHS tilt and rotation occurred at approximately .585 and 1.75 Hz. In each of the three planes, the trunk responds quite similarly to the MHS motion, as proven by earlier methods. However, it should be noted that in the transverse plane, the trunk has a slight response at 1.17 Hz, where the MHS is only moving in the sagittal plane. The gains were also quite similar across all planes and trials. The gains in the frontal and sagittal planes decreased as the frequency increased, but the opposite was true for the transverse plane. The lag was, on average, the least in the frontal plane, followed by the sagittal, then finally the transverse. As expected, the lag was also much larger in each plane for the higher frequencies.

Electromyography Data

EMG data was taken for all participants across all pre/post-exercises and riding trials. The muscles collected were on the left and ride side upper abdominals, lumbars, gluteus maximus, and lateral biceps femoris for a total of eight channels. Because there is a lack of EMG data collected while riding horses, this study sought to discover if there was any significant muscle activation while riding that would correspond to a good muscle building exercise. However, the data that was collected is very difficult to decipher due to the inconsistent nature of EMG collections. Multiple participants' EMG signals would cut in and out, rendering that data unreliable. From the little data that was obtained, it seemed that the abdominals and lumbar muscles do not get above 30% of the maximum voluntary isometric contractions, which is generally considered to be a significant muscle building exercise, which is a main goal of therapy [45,46]. Also, because the Noraxon EMG system was being run through the Vicon Nexus software, there was a delay between the EMG data and the motion capture data, but the delay was not consistent among participants or trials. The entirety of three riding trials for one participant who had reliable EMG data can be found in Appendix B. Also, the pre, post1, and post2 alternating hip extension EMG data for that participant can be found in Appendix C. In Figures 24-26, the data of the participant who had consistent EMG signals can be found for the left and right abs, lumbars, and glutes, respectively. Because Garner et al. analyzed the motion cycles of riding and walking, the EMG data shown is from pre-ride walking, the first trial of riding, and the first post-ride walk trial. Since the walk trials only consisted of a 15 foot walk across the motion lab, the first 5000 data points are shown in the graphs for all trials. The Noraxon system collected the data at

1200 Hz, therefore the total time elapsed is slightly more than four seconds. The MHS completes a full motion cycle every 1.7 seconds, so this means that about two and a half motion cycles are shown below in row two. From looking at the graphs, one can observe that the walking trials generally elicited a larger activation than riding from these muscle groups. It should also be noted that the large peaks in the ab graphs are heartbeat artifact. Because the EMG data was collected through the Vicon system rather than the Noraxon system, this was not able to be eliminated by the normal procedure.

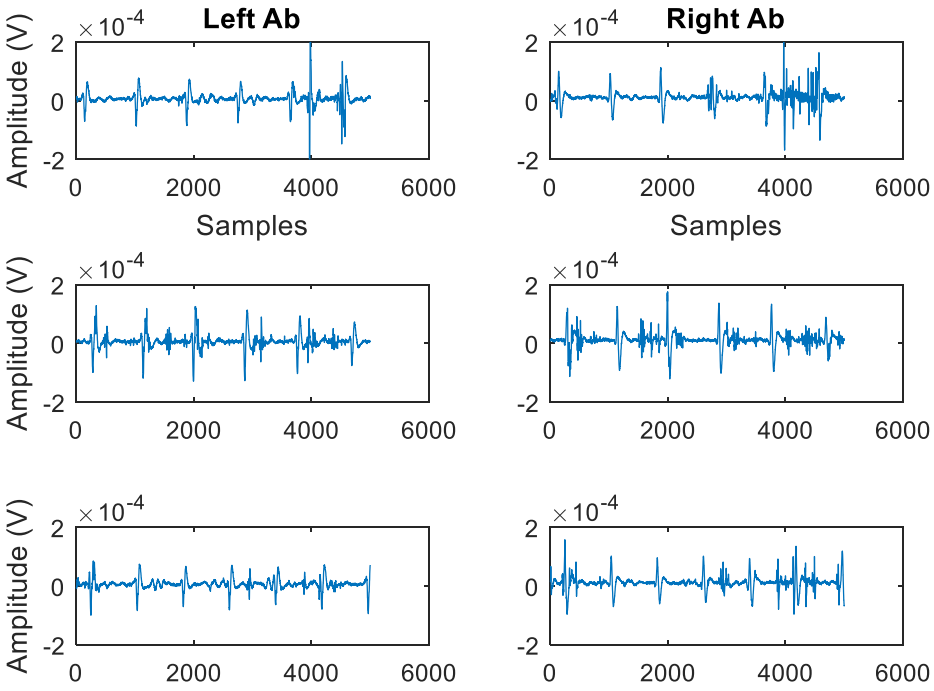

Figure 24: EMG Ab Data of One Participant. The first row is the pre-ride walk, the second row is the first riding trial, and the third row is the post-ride walk.

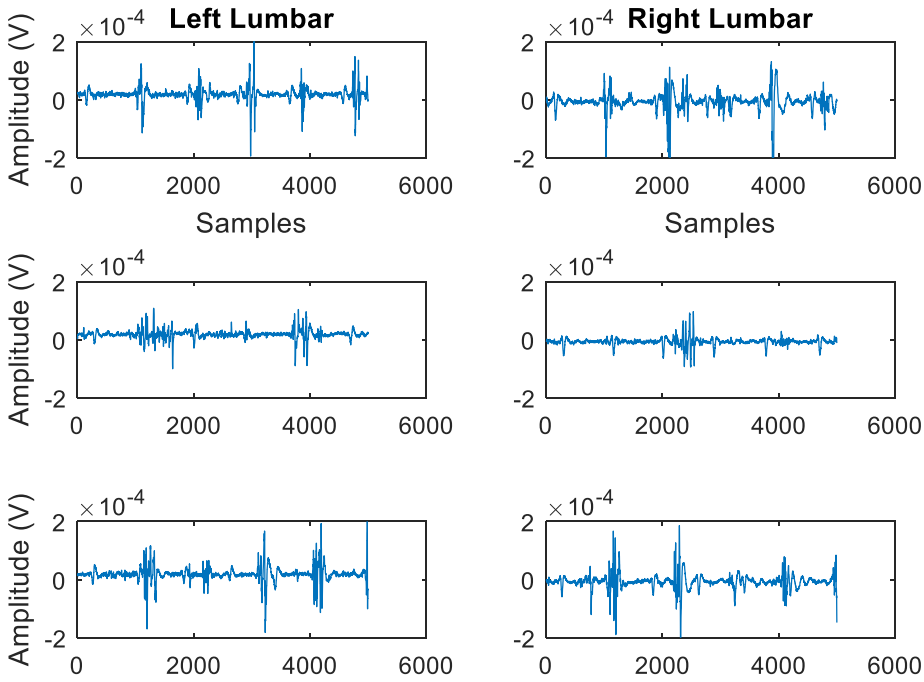

Figure 25: EMG Lumbar Data of One Participant. The first row is the pre-ride walk, the second row is the first riding trial, and the third row is the post-ride walk.

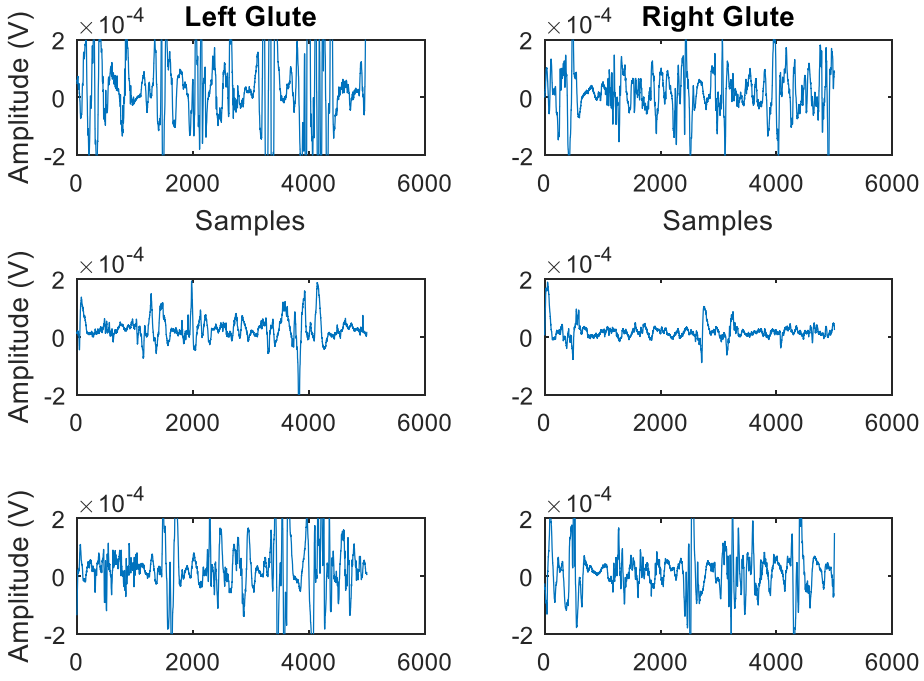

Figure 26: EMG Glute Data of One Participant. The first row is the pre-ride walk, the second row is the first riding trial, and the third row is the post-ride walk.

CHAPTER FOUR

Discussion

Significance

This study expanded on previous studies such as Garner et al. and Benoit et al., by adding in more accurate riding data/angles, pre/post-ride measures, and pilot EMG data [5,51]. Whereas Garner used four real horses to collect average riding motion, the current study used the MHS mechanical horse technology. While other studies focused on the pre/post effects of regular or simulated hippotherapy, this is the first study of its kind to evaluate how the rider responds to the imparted motion of the MHS. Many previous balance studies also evaluated the response to perturbations in one plane [13,49], but literature research for this study revealed no others that evaluated responses to perturbations in all three planes. It should also be noted that the motion of the MHS found in this study bears a striking resemblance to that of the motion of real horses in Garner's study [5]. This similarity suggests that physiological responses resulting from the riding motions of normal hippotherapy may also occur by use of the MHS. Also, the specificity of posture responses in planes and frequencies implies that one could simply adjust the frequency of the MHS motion to initiate specific desired responses. It is well known that each horse exhibits different three-dimensional patterns, but the mechanical horse could provide a variety of very specific motion patterns.

Pre/Post Test Balance

The p-values that were calculated between each of the balance tests did not show statistical significance, but there were clearly a few trends that can be seen in the data, even in healthy participants. One of the most notable trends is that during the two-legged closed eye balance tests, the participants tended to exhibit a high variability (> 8 mm) during the pre-ride balance tests, then that variability would decrease in one or both of the post-ride tests. It is unknown whether this is from the MHS perturbations or from increased practice throughout the collection.

Another important trend is that the average standard deviations in the y direction (sagittal) were nearly double those in the x (frontal). Our findings are supported by multiple previous studies that have also shown that humans are inherently less stable in the lateral direction [52,53]. Both CoP deviations decreased immediately after riding and increased five minutes later. Interestingly, more than 50% of the participants commented that they felt as if they were still twisting back and forth during the first immediate post-test balance, similar to that of the sensation of getting off a rocky boat. This might explain the large increase in moments about the z axis in Post1 balance test standard deviations. However, as the rider relaxed for a five minute break, their twisting moments decreased like the CoP measures, as shown in the Post2 tests. Another similar study tested balance before and after with two CP groups performing a 12-week hippotherapy programs: a group that used a real horse and one that used another mechanical horse on the market called the Panasonic Joba [54]. Both groups exercised one hour per day, three times per week, which is much longer than the riding trials in this study. They found that both groups significantly increased their balance through the use of the Pediatric Balance

Scale (PBS), but there was no significant difference between the two groups. This is a testament to the efficacy of hippotherapy and the possibility of using mechanical horses as a compliment to real horses. Our participants didn't show such increase in balance likely due to their being a healthy population to begin with, and only testing before and after one short riding session.

Single leg balance tests with eyes open over a 15 second period were also analyzed and the results for all participants can be found in Appendix D. However, these tests were much more variable between participants as well as between trials and therefore harder to find trends in the data. This could be because of the tougher nature of the task at hand. In addition to that, the test was much shorter (15 seconds as opposed to 60 seconds), so one small tilt could throw off the average standard deviation measures of the test.

Riding Data

The riding data showed that the motion of the healthy rider's trunk bore a striking resemblance to that of the mechanical horse with a slight delay, as shown in Figures 18-20. Table 1 shows that the rider motion was most correlated to the frontal plane horse motion, which is the mediolateral sway, and least correlated to the transverse motion, also known as the yaw. One explanation for the variance between planes is based on the different threat of injury. A previous posture study showed a significant difference in muscle activations and behavior due to postural threats such as being lifted high above the ground [43]. Because transverse plane is not affected by gravity, it is least important for posture and will not result in a fall. Therefore, its variability can be higher without the risk of injury. However, in the other two planes, a larger variability can result in a

higher risk of falling. Horses (and MHS) offer a small margin of error in the frontal plane as sliding laterally to one side or the other could result in literally falling off the horse. This could explain the small variance in the frontal plane due to the small margin of error. On the other hand, a fall in the sagittal plane would result in the rider falling on the front or back of the seat, which is a less threatening option, giving them more margin of error/variance in the sagittal plane. A previous study that applied visual and physical perturbations to people walking on a treadmill showed that participants were less stable in the sagittal plane than in the frontal plane [53]. Like this study shows while riding, the transverse plane has also been shown to be the most variable among walking patterns in both healthy and lower-back-injured populations [55,56]. These control processes across planes of motion along with the similarity between pelvic kinematics in riding and walking shown in Garner's study could be responsible for improving gait mechanics in disabled populations. The strong response in the frontal plane might also give us insight as to why the deviations in the CoPx decreased so dramatically immediately post-riding. The pattern in the sagittal plane was also very similar to saddle pressures reported in another hippotherapy study by Janura et al [57]. This same study showed that repeated hippotherapy practice can reduce variability in all planes. In the angle-angle plots (Figure 11), one can see that the trunk responds very similarly in all three planes and had the largest range of motion in the sagittal plane.

Posture responses in all three planes occurred at the same frequencies as those of the horse. Figures 21-23 show that the main frequencies were at 1.17 and 2.34 Hz for the sagittal plane and .585 and 1.756 Hz for the frontal and transverse. That is, the horse and rider were both moving twice as frequently in the frontal and transverse planes, due to

there being a full motion cycle in each of those planes for each left and each right phase of motion in the sagittal plane. The two main frequencies in the frontal and transverse planes were the same and although there was some sagittal plane response at these frequencies, it was minimal. Because the frontal and transverse planes responded at the same frequencies, an interaction between these two planes cannot be ruled out. Responses to frontal and sagittal plane stimuli have typically shown that gain usually increases in frequencies from .01 to .8 Hz, but begins to decrease at frequencies above 1 Hz [13,49]. This is backed up by data shown in figures 21-23 and shows that processes during single plane stimulus may also be applicable to more complex three-dimensional stimuli such as the MHS. This study did not evaluate gains in the transverse plane, but we found them to have the opposite trend of the other two planes as they increased with increasing frequency. This might be because trunk rotational inertia and biomechanical factors are very different than in the other two planes. Also, gravity does not affect the rotation in the transverse plane, but it does affect the tilt in both the sagittal and frontal planes. A previous study showed through modeling that low to mid-frequency (.2Hz – 2Hz) gains and phases are influenced mostly by sensory feedback, whereas higher frequency (> 2Hz) gains and phases are more influenced by reflexive processes and intrinsic biomechanics [49]. This means that the riders in this study were generally using sensory feedback, which is the desired outcome for the disabled riders because the goal is to have them respond to the horse motion with similar kinematics through the use of their own senses. The linear responses in this study are consistent with other posture studies that provided sway in only one plane [13,49].

The calculation of posture responses in this study was based on the horse tilt and rotation, but there were also small translations that could be detected by eye. These translations could slightly influence responses in the frontal and sagittal planes, but would not be expected to impact the transverse plane motion. Maximum translations in the x direction, which would affect the sagittal plane, were calculated to be.014 m, .1 m/s, and .85 m/s^2. The maximum translations in the y direction, which would affect the frontal plane, were .006 m, .035 m/s, and .35 m/s^2 [49].

The data provided gives us an idea of how we would like a disabled population to respond to the mechanical horse. From this, we can introduce therapeutic riding programs that would lead them closer to this "gold standard" of mechanical horse-induced motion. As we know from Garner's study, the motion imparted to the hips and trunk are very similar to that of a normal gait pattern, so by having the patients ride the horse for a multi-week program, we could effectively be "re-teaching" them how to properly use those muscles in proper firing order. The mechanical horse could be used to replicate the motion of multiple different horses just by the simply changing the frequency and pattern that it moves. Another interesting effect of the mechanical horse that was observed is that the larger the rider was, the slower the horse went and the smaller the range of amplitude was. This makes it more optimal for smaller people/children.

Electromyography

Originally, the electromyography was going to be the main focus of this study, but due to complications, it became an add-on to the motion capture data that was collected. Nonetheless, patterns can be seen in the small amount of EMG data that was

obtained. As one might expect in a nondisabled population, the walking patterns and EMG signals didn't change much in the pre and post-ride walking trials. However, the data shows similar patterns and activation levels between riding and walking in the lumbars and the abs. As for the glutes, they are activated much more during walking when compared to sitting on the horse.

Limitations of this Study

As with any study, this one had some limitations. Firstly, there was a small number of participants evaluated (N=11). Another was the lack of reliable EMG data. Due to running the Noraxon EMG system through the Vicon software, the plug-in and transfer caused for a delay between the motion capture and EMG data. For this reason, it was impossible to sync motion and muscular data together. Also for unknown reasons, the EMG would cut in and out of certain participants' trials, making it impossible to process all data the same way and find significant patterns across the population. This study was also limited by the fact that the riding session was only five minutes long as opposed to common riding therapy programs which are normally multiple sessions spanning over a few weeks [26,58]. This study only addressed the horse motion at one speed (slow walk), but to fully understand trunk adaptations, one could investigate the responses to different speeds as speed and amplitude might evoke changes in the posture control systems.

CHAPTER FIVE

Conclusion

Eleven healthy individuals responded to complex three-dimensional mechanical horse motion to prove the MHS is a very realistic mechanical horse that may be the future of hippotherapy. Unlike other simulators on the market, the MHS is capable of moving in all six degrees of freedom. It is also very affordable, space-efficient, and only requires a regular wall outlet to operate.

Although this study is only preliminary, it brings to light the great potential of the MHS mechanical horse technology. Unlike other similar studies that have proven the effects of real horseback riding, this is the first to evaluate kinematics during riding and pre/post-riding measures of a mechanical horse with six degrees of freedom. It first shows that with a rider on it, the MHS is capable of recreating a very similar pattern to a real horse walking motion. This study also portrays the changes in kinematics across a normal, five minute riding trial in a nondisabled population. Finally, the study shows that even in a nondisabled population, while there were not changes in the walking patterns, there are changes in the pre and post-ride balance trials. This suggests that these results would be even more pronounced in a disabled population, especially if tested over a longer riding program. The results given provide knowledge about trunk responses to complex stimuli in all three planes and a baseline for comparisons to pathological populations.

Future Work

Although there were a limited number of participants in this study, the amount of data that was collected is far from insignificant. From the data that has been collected from this study, more analysis could be performed on the pre/post-test measures to determine any differences in walking form, alternating hip extensions, or toe touches, but changes would not be expected to be seen in the healthy participants that were tested after only one five minute session of riding. Future studies could also record more reliable EMG data and determine the muscle firing rates, patterns of pre/post-test measures, and even fatigue while riding the MHS. Most importantly, future studies could include more participants with a healthy and disabled population who both go through a series of therapeutic riding sessions to evaluate the long-term effects of the mechanical horse and how the two groups compare.

APPENDICES

APPENDIX A

Matlab Code

Pre and Post Ride Processing File

```
clear
close all

kk=1; % this is the index for number of participants
for sub_num=1:11
for i=1:3
    if i==1
        test_num=1;
        eval(['load
BB_Subj',int2str(sub_num),'_PRE_NarrowBalance_TR01'])
    elseif i==2
        test_num=1;
        eval(['load
BB_Subj',int2str(sub_num),'_POST',int2str(test_num),'_NarrowBalance_TR0
1'])
    elseif i==3
        test_num=2;
        eval(['load
BB_Subj',int2str(sub_num),'_POST',int2str(test_num),'_NarrowBalance_TR0
1'])
    end

start_ind = 1; %start at 1001 frame (just in case)
end_ind = 73000; %60s +1000 frames (keep to 60s for all to standarize)

CoPx=table2array(ForcePlateData.Plate1.Center(start_ind:end_ind,3));
%CoP x
CoPy=table2array(ForcePlateData.Plate1.Center(start_ind:end_ind,4));
%CoP y
Mz=table2array(ForcePlateData.Plate1.Moment(start_ind:end_ind,5));
%moment about z
zCoPx=CoPx-CoPx(1);
zCoPy=CoPy-CoPy(1);

samprate=1200;
L=length(CoPx);
tmax=L/samprate;
t=linspace(0, tmax-1/samprate, samprate*tmax);

clf
subplot(221)
plot(t,CoPx)
title('CoPx')
subplot(222)
plot(t,CoPy)
```

```
title('CoPy')
subplot(223)
plot(t,Mz)
title('Mz')
%%pause

RMS_x(i,:)=std(CoPx,1);
RMS_y(i,:)=std(CoPy,1);
RMS_Mz(i,:)=std(Mz,1);
for pp=1:L
dist(i,pp) = sqrt(zCoPx(pp)^2+zCoPy(pp)^2);
end

RMSv_x(i,:)=std(cdiff(CoPx)*samprate,1);
RMSv_y(i,:)=std(cdiff(CoPy)*samprate,1);
RMSv_Mz(i,:)=std(cdiff(Mz)*samprate,1); %Common measures for balance

[yx,f]=dft(CoPx,samprate,200);
mag_yx = abs(yx);
[yy,f]=dft(CoPy,samprate,200);
mag_yy = abs(yy);
[ymz,f]=dft(Mz,samprate,200);
mag_mz = abs(ymz);

mag_yx_t(i,:)=mag_yx;
mag_yy_t(i,:)=mag_yy;
mag_Mz_t(i,:)=mag_mz;

emg_Lab1 = abs(EMGTable.EMGData{2,1});
emg_Rab1 = abs(EMGTable.EMGData{3,1});
emg_Llum1 = abs(EMGTable.EMGData{4,1});
emg_Rlum1 = abs(EMGTable.EMGData{5,1});
emg_Lglut1 = abs(EMGTable.EMGData{6,1});
emg_Rglut1 = abs(EMGTable.EMGData{7,1});

start_ind2=start_ind*1200/1200;
end_ind2=end_ind*1200/1200;

%take average of emg and then give to Cody
%take average across participants

emg_Lab(:,i) = emg_Lab1(start_ind2:end_ind2);
emg_Rab(:,i) = emg_Rab1(start_ind2:end_ind2);
emg_Llum(:,i) = emg_Llum1(start_ind2:end_ind2);
emg_Rlum(:,i) = emg_Rlum1(start_ind2:end_ind2);
emg_Lglut(:,i) = emg_Lglut1(start_ind2:end_ind2);
emg_Rglut(:,i) = emg_Rglut1(start_ind2:end_ind2);

clf
i=i+1;


end %End of all three test conditions
% Plots
clf
```

```
subplot(231)
bar(RMS_x); title(['S=',int2str(sub_num),'RMSCoPx'])
subplot(232)
bar(RMS_y); title('RMS CoPy')
subplot(233)
bar(RMS_Mz); title('RMS Mz')
subplot(234)
bar(RMSv_x); title('RMSv CoPx')
subplot(235)
bar(RMSv_y); title('RMSv CoPy')
subplot(236)
bar(RMSv_Mz); title('RMSv Mz')


% Collect data across participants
mag_yx_t_all(:,:,kk) = mag_yx_t;
mag_yy_t_all(:,:,kk) = mag_yy_t;
mag_Mz_t_all(:,:,kk) = mag_Mz_t;

RMS_x_all(:,kk) = RMS_x;
RMS_y_all(:,kk) = RMS_y;
dist_all(:,kk) = mean(dist,2);

RMSv_x_all(:,kk) = RMSv_x;
RMSv_y_all(:,kk) = RMSv_y;

emg_Lab_all(:,kk)= mean(emg_Lab);
emg_Rab_all(:,kk)= mean(emg_Rab);
emg_Llum_all(:,kk)= mean(emg_Llum);
emg_Rlum_all(:,kk)= mean(emg_Rlum);
emg_Lglut_all(:,kk)= mean(emg_Lglut);
emg_Rglut_all(:,kk)= mean(emg_Rglut);

kk=kk+1;
end
%% make average time domain measures
clf
clear aRMS_x
for ii=1:3
subplot(231)
aRMS_x = mean(RMS_x_all(ii,:));
sRMS_x = std(RMS_x_all(ii,:));
bar(ii,aRMS_x); hold on
errorbar(ii,aRMS_x,sRMS_x)
title('CoP RMSx')

subplot(232)
aRMS_y = mean(RMS_y_all(ii,:));
sRMS_y = std(RMS_y_all(ii,:));
bar(ii,aRMS_y); hold on
errorbar(ii,aRMS_y,sRMS_y)
title('CoP RMSy')

subplot(233)
aRMS_Mz = mean(mag_Mz_t_all(ii,:));
```

```
sRMS_Mz = std(mag_Mz_t_all(ii,:));
bar(ii,aRMS_Mz); hold on
errorbar(ii,aRMS_Mz,sRMS_Mz)
title('CoP RMS Mz')

subplot(234)
aRMSv_x = mean(RMSv_x_all(ii,:));
sRMSv_x = std(RMSv_x_all(ii,:));
bar(ii,aRMSv_x); hold on
errorbar(ii,aRMSv_x,sRMSv_x)
title('CoP RMSv x')

subplot(235)
aRMSv_y = mean(RMSv_y_all(ii,:));
sRMSv_y = std(RMSv_y_all(ii,:));
bar(ii,aRMSv_y); hold on
errorbar(ii,aRMSv_y,sRMSv_y)
title('CoP RMSv y')

subplot(236)
adist = mean(dist_all(ii,:));
sdist = std(dist_all(ii,:));
bar(ii,adist); hold on
errorbar(ii,adist,sdist)
title('CoP distance')
end


%% make average amp specta
%I would expect to see an after-effect in
%in x at f=1.17Hz (pt 70/71)& 2.34Hz.
%in y at f=0.585 (pt 35) & 1.75.
% in transver same as y
% so I'm only looking at sway at (or near) these discrete
% frequencies.  I already looked across the whole spectra and did not
see
% much
clf
clear a_mag_yx2 a_mag_yy2 a_mag_Mz2 a_mag_yx a_mag_yy a_mag_Mz
for ii=1:3
    figure(3)
    %discrete pts
a_mag_yx2(ii) = mean(mean(mag_yx_t_all(ii,70:71,:),3));
a_mag_yy2(ii) = mean(mag_yy_t_all(ii,35,:),3);
a_mag_Mz2(ii) = mean(mag_Mz_t_all(ii,35,:),3);
    %whole spectra
a_mag_yx(ii,:) = mean(mag_yx_t_all(ii,:,:),3);
a_mag_yy(ii,:) = mean(mag_yy_t_all(ii,:,:),3);
a_mag_Mz(ii,:) = mean(mag_Mz_t_all(ii,:,:),3);

% subplot(231)
% bar(f,a_mag_yx(ii,:)); title('Amp CoPx')
% hold on
% subplot(232)
% bar(f,a_mag_yy(ii,:)); title('Amp CoPy')
% hold on
```

```
% subplot(233)
% bar(f,a_mag_Mz(ii,:)); title('Amp Mz')
% hold on

subplot(131)
bar(ii,a_mag_yx2(ii)); title('Amp CoPx')
hold on
subplot(132)
bar(ii,a_mag_yy2(ii)); title('Amp CoPy')
hold on
subplot(133)
bar(ii,a_mag_Mz2(ii)); title('Amp Mz')
hold on

end
```

Single Participant Analysis File

```
clear
close all

%Subj#, TR01,02,03 and Ride1,2,3
%Subj#_AD_, Pelvis or PelvisAndTrunk or Control or Trunk
for test_type=1
for sub_num=11
    if test_type==1
        test_num_tally=[1:3];
    elseif test_type==2
         test_num_tally=[1:5];
    end

for test_num=test_num_tally

    if test_type==1
eval(['load BB_Subj',int2str(sub_num),'_Ride_TR0',int2str(test_num)])
eval(['load
Subj',int2str(sub_num),'_Ride',int2str(test_num),'_Horse.txt'])
eval(['Ridefun2=
Subj',int2str(sub_num),'_Ride',int2str(test_num),'_Horse;'])
    elseif test_type==2
eval(['load BB_Subj',int2str(sub_num),'_AD_',int2str(test_num)])
eval(['load
Subj',int2str(sub_num),'_AD_',int2str(test_num),'_Horse.txt'])
eval(['Ridefun2=
Subj',int2str(sub_num),'_AD_',int2str(test_num),'_Horse;'])
    end

%%
%load BB_Subj2_Ride_TR03
% load Subj2_Ride3_horse.txt
%Ridefun=Subj2_Ride3_horse;
funpoint = trajectories{5,1};
funpointx = table2array(funpoint(:,1));
samprate=120;
L2=length(funpointx); %num of points
Lt = L2/samprate; %total time of test (s)

start_index=1;
end_index=L2;
if test_type == 2 && sub_num == 2 && test_num == 4
    start_index = 81
end
if test_type == 2 && sub_num == 2 && test_num == 5
    start_index = 26
end
if test_type == 2 && sub_num == 2 && test_num == 5
    end_index = 1600
end
if test_type == 2 && sub_num == 3 && test_num == 1
    start_index = 42
end
if test_type == 2 && sub_num == 3 && test_num == 5
```

```
    end_index = 6090
end
if test_type == 2 && sub_num == 4 && test_num == 5
    start_index = 8
    Ridefun2 = [zeros(7,12);Ridefun2];
end
if test_type == 1 && sub_num == 5 && test_num == 1
    end_index = 2520
    Ridefun2 = [Ridefun2;zeros(1,12)];
end
if test_type == 2 && sub_num == 5 && test_num == 1
    start_index = 55
end
if test_type == 2 && sub_num == 5 && test_num == 2
    start_index = 9;
    Ridefun2 = [zeros(8,12);Ridefun2];
end
if test_type == 2 && sub_num == 8 && test_num == 3
    start_index = 2
end
if test_type == 2 && sub_num == 7 && test_num == 2
    start_index = 3;
    end_index = 6000;
    Ridefun2 = [zeros(2,12);Ridefun2;zeros(6,12)];
end
if test_type == 1 && sub_num == 6 && test_num == 1
    start_index = 8;
    Ridefun2 = [zeros(7,12);Ridefun2];
end
if test_type == 1 && sub_num == 6 && test_num == 2
    start_index = 23;
    Ridefun2 = [zeros(22,12);Ridefun2];
end
if test_type == 2 && sub_num == 8 && test_num == 2
    end_index = 6500
end
if test_type == 2 && sub_num == 8 && test_num == 3
    end_index = 4000
end
if test_type == 2 && sub_num == 8 && test_num == 4
    end_index = 2500
end
if test_type == 2 && sub_num == 7 && test_num == 3
    start_index = 3
    end_index = 4499
end
if test_type == 2 && sub_num == 7 && test_num == 4
    start_index = 14
    end_index = 7317
end
if test_type == 2 && sub_num == 7 && test_num == 5
    start_index = 13
end
if test_type == 1 && sub_num == 1 && test_num == 1
    start_index = 12;
    Ridefun2 = [zeros(11,12);Ridefun2];
end
```

```
if test_type == 2 && sub_num == 9 && test_num == 1
    start_index = 450
    end_index = 3500
end
if test_type == 2 && sub_num == 9 && test_num == 3
    start_index = 1800
end
if test_type == 2 && sub_num == 9 && test_num == 4
    end_index = 3400
end
L=end_index-start_index+1;

t = linspace(0,L/samprate,L);
{'LASI';'RASI';'LPSI';'RPSI'};
% LASI_pos = trajectories{24,1};
% LASIx=table2array(LASI_pos(start_index:end_index,1));
% LASIy=table2array(LASI_pos(start_index:end_index,2));
% LASIz=table2array(LASI_pos(start_index:end_index,3));
%
% RASI_pos = trajectories{25,1};
% RASIx=table2array(RASI_pos(start_index:end_index,1));
% RASIy=table2array(RASI_pos(start_index:end_index,2));
% RASIz=table2array(RASI_pos(start_index:end_index,3));

LPSI_pos = trajectories{26,1};
LPSIx=table2array(LPSI_pos(start_index:end_index,1));
LPSIy=table2array(LPSI_pos(start_index:end_index,2));
LPSIz=table2array(LPSI_pos(start_index:end_index,3));

RPSI_pos = trajectories{27,1};
RPSIx=table2array(RPSI_pos(start_index:end_index,1));
RPSIy=table2array(RPSI_pos(start_index:end_index,2));
RPSIz=table2array(RPSI_pos(start_index:end_index,3));

LSho_pos = trajectories{10,1};
LShox=table2array(LSho_pos(start_index:end_index,1));
LShoy=table2array(LSho_pos(start_index:end_index,2));
LShoz=table2array(LSho_pos(start_index:end_index,3));

if test_type == 1 && sub_num == 5 && test_num < 4
    RSho_pos = LSho_pos;
    RShox = LShox;
    RShoy = LShoy;
    RShoz = LShoz;
else
    RSho_pos = trajectories{17,1};
    RShox=table2array(RSho_pos(start_index:end_index,1));
    RShoy=table2array(RSho_pos(start_index:end_index,2));
    RShoz=table2array(RSho_pos(start_index:end_index,3));
end

C7_pos = trajectories{5,1};
C7x=table2array(C7_pos(start_index:end_index,1));
C7y=table2array(C7_pos(start_index:end_index,2));
C7z=table2array(C7_pos(start_index:end_index,3));
Ridefun=Ridefun2(start_index:end_index,:);
```

```
%% here is a version that only looks at PSIS and Shoulders and
autofills zeros
count=0;
for i=1:L
 if LPSIx(i)==0
     LPSIx(i)=LPSIx(i-1);
     LPSIy(i)=LPSIy(i-1);
     LPSIz(i)=LPSIz(i-1);
 count=count+1;
 end
end
count

count=0;
for i=1:L
 if LShox(i)==0
     LShox(i)=LShox(i-1);
     LShoy(i)=LShoy(i-1);
     LShoz(i)=LShoz(i-1);
 count=count+1;
 end

end
count

%% here is a version that only looks at PSIS and Shoulders and
autofills zeros
count=0;
for i=1:L
 if RPSIx(i)==0
     RPSIx(i)=RPSIx(i-1);
     RPSIy(i)=RPSIy(i-1);
     RPSIz(i)=RPSIz(i-1);
 count=count+1;
 end
end
count

count=0;
for i=1:L
 if RShox(i)==0
     RShox(i)=RShox(i-1);
     RShoy(i)=RShoy(i-1);
     RShoz(i)=RShoz(i-1);
 count=count+1;
 end
end
count

%% Define mid-point of pelvis and shoulders
mPelvisx = (RPSIx+LPSIx)/2;
mPelvisy = (RPSIy+LPSIy)/2;
mPelvisz = (RPSIz+LPSIz)/2;
```

```
if test_type == 1 && sub_num == 5 && test_num < 4
    mShox = C7x;
    mShoy = C7y;
    mShoz = C7z;
else
    mShox = (RShox+LShox)/2;
    mShoy = (RShoy+LShoy)/2;
    mShoz = (RShoz+LShoz)/2;
end

subplot(321)
plot(t,mPelvisx,'k'); hold on
% plot(t,RPSIx,'r')
% plot(t,LPSIx,'r')

title('Pelvis x,y,z')
subplot(323)
plot(t,mPelvisy,'k')
subplot(325)
plot(t,mPelvisz,'k')

subplot(322)
plot(t,mShox,'k')
title('Shoulder x,y,z')

subplot(324)
plot(t,mShoy,'k')
subplot(326)
plot(t,mShoz,'k')
pause
clf


%% Looking at horse stuff
%marker order is 1, 2, 4, 3
%marker meaning is 1=front right; 2=back right; 3=back left; 4=front
left
if sub_num ==6
    mid_horsex=(Ridefun(:,4)+Ridefun(:,7))/2;
    mid_horsey=(Ridefun(:,5)+Ridefun(:,8))/2;
    mid_horsez=(Ridefun(:,6)+Ridefun(:,9))/2;
else

mid_horsex=(Ridefun(:,1)+Ridefun(:,4)+Ridefun(:,7)+Ridefun(:,10))/4;

mid_horsey=(Ridefun(:,2)+Ridefun(:,5)+Ridefun(:,8)+Ridefun(:,11))/4;

mid_horsez=(Ridefun(:,3)+Ridefun(:,6)+Ridefun(:,9)+Ridefun(:,12))/4;
end
% subplot(311)
% plot(mid_horsex)
% title('midpt of horse x,y,z')
% subplot(312)
% plot(mid_horsey)
```

```
% subplot(313)
% plot(mid_horsez)
% pause

% Now do angle (sagittal plane) pitch
if sub_num == 66
    f_a_horse = (Ridefun(:,1:3));
    midx6 = (Ridefun(:,1)+Ridefun(:,4))/2;
    midz6 = (Ridefun(:,3)+Ridefun(:,6))/2;
    sag_horse = atand((f_a_horse(:,3)-midz6)./(f_a_horse(:,1)-midx6));
    sag_horse_zm = sag_horse-mean(sag_horse);
else
    f_a_horse = (Ridefun(:,1:3)+Ridefun(:,7:9))/2;
    sag_horse = atand((f_a_horse(:,3)-mid_horsez)./(f_a_horse(:,1)-
mid_horsex));
    sag_horse_zm=sag_horse-mean(sag_horse);
end
% plot(sag_horse_zm,'b')
% hold on
% half_x_horse=(mean(Ridefun(:,1))+mean(Ridefun(:,7)))/2-
mean(mid_horsex);
% sag_horse = asind((f_a_horse(:,3)-mid_horsez)./(half_x_horse));
% sag_horse_zm=sag_horse-mean(sag_horse);
% plot(sag_horse_zm,'-r')

%Frontal Roll
if sub_num == 66
    f_b_horse = (Ridefun(:,1:3));
    midy6 = (Ridefun(:,2)+Ridefun(:,8));
    midz6f = (Ridefun(:,3)+Ridefun(:,9));
    fron_horse = atand((f_b_horse(:,3)-midz6f)./(f_b_horse(:,2)-
midy6));
    fron_horse_zm = fron_horse-mean(fron_horse);
else
    f_b_horse = (Ridefun(:,1:3)+Ridefun(:,4:6))/2;
    fron_horse = atand((f_b_horse(:,3)-mid_horsez)./(f_b_horse(:,2)-
mid_horsey));
    fron_horse_zm = fron_horse-mean(fron_horse);
end
% plot(fron_horse_zm,'b')
% hold on
% half_y_horse = (mean(Ridefun(:,2))+mean(Ridefun(:,5)))/2-
mean(mid_horsey);
% fron_horse = asind((f_b_horse(:,3)-mid_horsez)./half_y_horse);
% fron_horse_zm = fron_horse-mean(fron_horse);
% plot(fron_horse_zm,'r')

%Transverse Yaw
tran_horse = atand((f_a_horse(:,2)-mid_horsey)./(f_a_horse(:,1)-
mid_horsex));
tran_horse_zm = tran_horse-mean(tran_horse);



%% Trunk sway (tilt angle of C7 wrt pelvis) & Shoulder yaw & Pelvis
roll/pitch
```

```
% now do a quick estimate of pelvis tilt in Frontal and Saggittal
zf = 115;%estimated difference seat (under butt) to markers on horse
h_pel = mean(mPelvisz)-mean(mid_horsez) - zf;
h_c7_pel = ((C7x-mPelvisx).^2 + (C7y-mPelvisy).^2 + (C7z-
mPelvisz).^2).^.5;
h_shoulders = ((LShox-RShox).^2 + (LShoy-RShoy).^2 + (LShoz-
RShoz).^2).^.5;
w_pel = ((RPSIx-LPSIx).^2 + (LPSIy-RPSIy).^2).^.5;
half_pel = mean(w_pel)/2;
w_pel_f = ((RPSIz-LPSIz).^2 + (LPSIy-RPSIy).^2).^.5;
half_pelf = mean(w_pel_f)/2;

mPelvis_x_zm = mPelvisx-mean(mPelvisx);
mPelvis_y_zm = mPelvisy-mean(mPelvisy);
mid_horsex_zm = mid_horsex-mean(mid_horsex)+zf*sind(sag_horse_zm);
%alternatively, sag_horse for non-zeroed
%mid_horsex_zm1 = mid_horsex++zf*sind(sag_horse_zm);
%mid_horsex_zm = mid_horsex_zm-mean(mid_horsex_zm);
%mid_horsey_zm = mid_horsey-mean(mid_horsey)+zf*sind(fron_horse_zm);
mPelvis_sag = asind((mPelvis_x_zm-mid_horsex_zm)./h_pel);
% mPelvis_fron = asind((mPelvis_y_zm-mid_horsey_zm)./h_pel);

mPelvis_fron2 = asind((RPSIz-mPelvisz)./half_pel);
mPelvis_fron = mPelvis_fron2-mean(mPelvis_fron2);

plot(h_c7_pel,'k'); hold on
plot(h_shoulders,'b')
title('C7 to pelvis and distance between Shoulders')
legend('C7 to Pelvis', 'Distance between Shoulders')
pause
clf

%
C7_sag = asind((C7x-mPelvisx)./h_c7_pel);
C7_sag_zm = C7_sag-mean(C7_sag);
subplot(221)
plot(C7_sag_zm)
title('C7 Sag')
ylabel('deg')

C7_fron = asind((C7y-mPelvisy)./h_c7_pel);
C7_fron_zm = C7_fron-mean(C7_fron);
subplot(222)
plot(C7_fron_zm)
title('C7 Front')
ylabel('deg')

Pelvis_tran = asind((RPSIx-mPelvisx)./half_pel);
Pelvis_tran_zm = Pelvis_tran-mean(Pelvis_tran);
subplot(223)
plot(Pelvis_tran_zm)
title('Pelvis Transv')
ylabel('deg')
```

```
if test_type == 1 && sub_num == 5 && test_num < 4
    half_sho = mean(LShoy - C7y);
    Sho_tran = -asind((RShox-mShox)./(half_sho));
    Sho_tran_zm = Sho_tran-mean(Sho_tran);
else
    half_sho = mean(h_shoulders)/2;
    Sho_tran = asind((RShox-mShox)./(half_sho));
    Sho_tran_zm = Sho_tran-mean(Sho_tran);
end

subplot(224)
plot(Sho_tran_zm)
title('Shoulder Transv')
ylabel('deg')
pause

%% angle - angle
clf
subplot(321)
plot(C7_sag_zm, C7_fron_zm)
xlabel('C7 Sagittal')
ylabel('C7 Frontal')
subplot(323)
plot(Sho_tran_zm, C7_fron_zm)
xlabel('Shoulder Transverse')
ylabel('C7 Frontal')
subplot(325)
plot(Sho_tran_zm, C7_sag_zm)
xlabel('Shoulder Transverse')
ylabel('C7 Sagittal')

subplot(322)
plot(sag_horse_zm, fron_horse_zm)
xlabel('Horse Sagittal')
ylabel('Horse Frontal')
subplot(324)
plot(tran_horse_zm, fron_horse_zm)
xlabel('Horse Transverse')
ylabel('Horse Frontal')
subplot(326)
plot(tran_horse_zm, sag_horse_zm)
xlabel('Horse Transverse')
ylabel('Horse Sagittal')
pause

%% Now find average cycle
%define cycle length on  frontal plane motin (zero crossing of filtered
%data) - arbitrary

[b,a]=butter(2,.07); %low pass 10 hz = 10/60, where 60 is 1/2 samprate
fron_horse_zm_f = filter(b,a,fron_horse_zm);
res=10^-2;
clear zero_cr
clf
ii=0;
```

```
for i=1:L-1
    if fron_horse_zm_f(i)<0 && fron_horse_zm_f(i+1)>0
        ii=ii+1;
        zero_cr(ii)=i;
    end
end
zero_cr;

% This is a nice plot of the zero crossing
plot(t,fron_horse_zm_f); hold on
scatter(t(zero_cr),fron_horse_zm_f(zero_cr),'o','r')
pause

clear poop fron_horse_zm_tally C7_fron_zm_tally sag_horse_zm_tally
C7_sag_zm_tally tran_horse_zm_tally
clear Sho_tran_zm_tally Pelvis_tran_zm_tally

for i=1:length(zero_cr)-1
poop(i)=(zero_cr(i+1)-zero_cr(i)); %finds number of frames between zero
crossings
end

ave_cyc_L_test = round(mean(poop)); %estimated average number of frames
for each cycle
ave_cyc_L = 205; %this is based on a 60 s trial and fixed so everyone
has the same cycle length to make averaging easier

    if abs(ave_cyc_L_test - ave_cyc_L) > 2
  error('look closer at your cycle length') %just a check to be sure
zero crossing make sense
    end

    %run participant 1-8 only do test 1 and get 8 numbers: stick into
excel (or
    %on a paper) and see how different they are  - is it better to use
206
    %than 205 (what is the average across all participant) - is my
daughher a
    %lot different than the rest?

ave_cyc_L_test
pause

start_cyc = zero_cr(1); %starting frame
tot_cycs = length(zero_cr); %total number of cycles to average across
tk = linspace(0,ave_cyc_L/samprate,ave_cyc_L); %time vector for
kinematics

% if sub_num==5 && test_num==1 && test_type==1
%     tot_cycs=13;
% end


% Here is a dft plot for your thesis...and for Brian
clf
```

```
subplot(311)
[y_tf,f]=dft(fron_horse_zm(start_cyc:start_cyc+(tot_cycs-1)*206-
1),120,250);
%[y_tf,f]=dft(fron_horse_zm(68:7061),120,250);
stem(f,abs(y_tf),'b'); hold on
set(gca,'xscal','log')
xlim([0.005 5])
title(['front plane amp spectra'])
ylabel('deg')
subplot(312)
[y_ts,f]=dft(sag_horse_zm(start_cyc:start_cyc+(tot_cycs-1)*206-
1),120,250);
%[y_ts,f]=dft(fron_horse_zm(68:7061),120,250);
stem(f,abs(y_ts),'b'); hold on
set(gca,'xscal','log')
xlim([0.005 5])
title(['sag plane amp spectra'])
ylabel('deg')
subplot(313)
[y_tt,f]=dft(tran_horse_zm(start_cyc:start_cyc+(tot_cycs-1)*205-
1),120,250);
%[y_tt,f]=dft(fron_horse_zm(68:7061),120,250);
stem(f,abs(y_tt),'b'); hold on
set(gca,'xscal','log')
xlim([0.005 5])
title(['trans plane amp spectra'])
ylabel('deg')
pause
%%

%loop below cycles through cycles and get kinematics for future
averaging
for i=0:tot_cycs-2
  fron_horse_zm_tally(i+1,:) =
fron_horse_zm(start_cyc+i*ave_cyc_L:start_cyc+(i+1)*ave_cyc_L-1);
  C7_fron_zm_tally(i+1,:) =
C7_fron_zm(start_cyc+i*ave_cyc_L:start_cyc+(i+1)*ave_cyc_L-1);
  sag_horse_zm_tally(i+1,:) =
sag_horse_zm(start_cyc+i*ave_cyc_L:start_cyc+(i+1)*ave_cyc_L-1);
  C7_sag_zm_tally(i+1,:) =
C7_sag_zm(start_cyc+i*ave_cyc_L:start_cyc+(i+1)*ave_cyc_L-1);
  tran_horse_zm_tally(i+1,:) =
tran_horse_zm(start_cyc+i*ave_cyc_L:start_cyc+(i+1)*ave_cyc_L-1);
  Sho_tran_zm_tally(i+1,:) =
Sho_tran_zm(start_cyc+i*ave_cyc_L:start_cyc+(i+1)*ave_cyc_L-1);
  Pelvis_tran_zm_tally(i+1,:) =
Pelvis_tran_zm(start_cyc+i*ave_cyc_L:start_cyc+(i+1)*ave_cyc_L-1);
  Pelvis_sag_tally(i+1,:) =
mPelvis_sag(start_cyc+i*ave_cyc_L:start_cyc+(i+1)*ave_cyc_L-1);
  Pelvis_fron_tally(i+1,:) =
mPelvis_fron(start_cyc+i*ave_cyc_L:start_cyc+(i+1)*ave_cyc_L-1);
end

%Frontal Roll of Horse vs C7
mHorse_F = mean(fron_horse_zm_tally,1);
sHorse_F = std(fron_horse_zm_tally);
```

```
subplot(221)
plot(tk,mHorse_F); hold on
% plot(tk,mHorse_F+sHorse_F,'y')
% plot(tk,mHorse_F-sHorse_F,'y')
title('Frontal Roll Horse vs Trunk')

mTrunk_F = mean(C7_fron_zm_tally,1);
sTrunk_F = std(C7_fron_zm_tally);

plot(tk,mTrunk_F);
% plot(tk,mTrunk_F+sTrunk_F,'g')
% plot(tk,mTrunk_F-sTrunk_F,'g')
legend('Horse', 'Trunk')
hold off

%Frontal Roll of Pelvis
mPelvis_F = mean(Pelvis_fron_tally);
sPelvis_F = std(Pelvis_fron_tally);

%Sagittal Pitch of Horse vs C7
mHorse_S = mean(sag_horse_zm_tally,1);
sHorse_S = std(sag_horse_zm_tally);

subplot(222)
plot(tk,mHorse_S); hold on
% plot(tk,mHorse_S+sHorse_S,'y')
% plot(tk,mHorse_S-sHorse_S,'y')
title('Sagittal Pitch Horse vs Trunk')

mTrunk_S = mean(C7_sag_zm_tally,1);
sTrunk_S = std(C7_sag_zm_tally);

plot(tk,mTrunk_S);
% plot(tk,mTrunk_S+sTrunk_S,'g')
% plot(tk,mTrunk_S-sTrunk_S,'g')
legend('Horse', 'Trunk')
hold off

%Sagittal Pitch of Pelvis
mPelvis_S = mean(Pelvis_sag_tally);
sPelvis_S = std(Pelvis_sag_tally);

%Transverse Yaw of Horse vs Shoulders
mHorse_T = mean(tran_horse_zm_tally,1);
sHorse_T = std(tran_horse_zm_tally);

subplot(223)
plot(tk,mHorse_T); hold on
% plot(tk,mHorse_T+sHorse_T,'y')
% plot(tk,mHorse_T-sHorse_T,'y')
title('Yaw Horse vs Shoulders')
mSho_T = mean(Sho_tran_zm_tally,1);
sSho_T = std(Sho_tran_zm_tally);
```

```
plot(tk,mSho_T); hold on
% plot(tk,mSho_T+sSho_T,'g')
% plot(tk,mSho_T-sSho_T,'g')
legend('Horse', 'Trunk')

%Transverse Yaw of Horse vs Pelvis
mHorse_T = mean(tran_horse_zm_tally,1);
sHorse_T = std(tran_horse_zm_tally);

subplot(224)
plot(tk,mHorse_T); hold on
% plot(tk,mHorse_T+sHorse_T,'y')
% plot(tk,mHorse_T-sHorse_T,'y')
title('Yaw Horse vs Pelvis')

mPelvis_T = mean(Pelvis_tran_zm_tally,1);
sPelvis_T = std(Pelvis_tran_zm_tally);

plot(tk,mPelvis_T,'k'); hold on
% plot(tk,mPelvis_T+sPelvis_T,'g')
% plot(tk,mPelvis_T-sPelvis_T,'g')
legend('Horse', 'Trunk')
pause

%Sagittal of Pelvis vs Horse
subplot(211)
plot(tk,mHorse_S); hold on
title('Sagittal Horse vs Pelvis')
plot(tk,mHorse_S+sHorse_S,'y')
plot(tk,mHorse_S-sHorse_S,'y')
plot(tk,mPelvis_S);
plot(tk,mPelvis_S+sPelvis_S,'g')
plot(tk,mPelvis_S-sPelvis_S,'g')
hold off

%Frontal of Pelvis and Horse
subplot(212)
plot(tk,mHorse_F); hold on
title('Frontal Horse vs Pelvis')
plot(tk,mHorse_F+sHorse_F,'y')
plot(tk,mHorse_F-sHorse_F,'y')
plot(tk,mPelvis_F);
plot(tk,mPelvis_F+sPelvis_F,'g')
plot(tk,mPelvis_F-sPelvis_F,'g')

[acorf,lagf] = xcorr(mHorse_F(1,:),mTrunk_F(1,:),'coeff');
[acors,lags] = xcorr(mHorse_S(1,:),mTrunk_S(1,:),'coeff');
[acort,lagt] = xcorr(mHorse_T(1,:),mSho_T(1,:),'coeff');

Fron_corr = max(acorf)
Sag_corr = max(acors)
Tran_corr = max(acort)
Fron_cor = mean(acorf)
Sag_cor = mean(acors)
```

```
Tran_cor = mean(acort)
pause

%% Average Angle-Angle Plots

% clf
% subplot(321)
% title('Angle vs Angle Plots')
% plot(mTrunk_S, mTrunk_F)
% xlabel('Avg C7 Sagittal')
% ylabel('Avg C7 Frontal')
% subplot(323)
% plot(mSho_T, mTrunk_F)
% xlabel('Avg Shoulder Transverse')
% ylabel('Avg C7 Frontal')
% subplot(325)
% plot(mSho_T, mTrunk_S)
% xlabel('Avg Shoulder Transverse')
% ylabel('Avg C7 Sagittal')

subplot(311)
plot(mHorse_S, mHorse_F,mTrunk_S, mTrunk_F)
xlabel('Avg Sagittal')
ylabel('Avg Frontal')
legend('Horse', 'Trunk')
subplot(312)
plot(mHorse_T, mHorse_F,mSho_T, mTrunk_F)
xlabel('Avg Transverse')
ylabel('Avg Frontal')
legend('Horse', 'Trunk')
subplot(313)
plot(mHorse_T, mHorse_S,mSho_T, mTrunk_S)
xlabel('Avg Transverse')
ylabel('Avg Sagittal')
legend('Horse', 'Trunk')
pause


%% EMG STUFF
%ave_cyc_Le = round(mean(poop))/120*1500; %number of frames / cycle in
emg
ave_cyc_Le = round(205/120*1500);
start_cyce = round(zero_cr(1)/120*1500); %frame number to start at (ie,
first zero crossing) in emg sampling rate
%tot_cycs = length(zero_cr); %commenting out because previously defined

emg_Lab = (EMGTable.EMGData{2,1});
emg_Rab = (EMGTable.EMGData{3,1});
emg_Llum = (EMGTable.EMGData{4,1});
emg_Rlum = (EMGTable.EMGData{5,1});
emg_Lglut = (EMGTable.EMGData{6,1});
emg_Rglut = (EMGTable.EMGData{7,1});
emg_Lham = (EMGTable.EMGData{8,1});
emg_Rham = (EMGTable.EMGData{9,1});
subplot(421)
plot(emg_Lab)
```

```
xlabel('Samples')
ylabel('Amplitude (V)')
title('Left Ab')
subplot(422)
plot(emg_Rab)
xlabel('Samples')
ylabel('Amplitude (V)')
title('Right Ab')
subplot(423)
plot(emg_Llum)
xlabel('Samples')
ylabel('Amplitude (V)')
title('Left Lumbar')
subplot(424)
plot(emg_Rlum)
xlabel('Samples')
ylabel('Amplitude (V)')
title('Right Lumbar')
subplot(425)
plot(emg_Lglut)
xlabel('Samples')
ylabel('Amplitude (V)')
title('Left Glute')
subplot(426)
plot(emg_Rglut)
xlabel('Samples')
ylabel('Amplitude (V)')
title('Right Glute')
subplot(427)
plot(emg_Lham)
xlabel('Samples')
ylabel('Amplitude (V)')
title('Left Hamstring')
subplot(428)
plot(emg_Rham)
xlabel('Samples')
ylabel('Amplitude (V)')
title('Right Hamstring')
pause
%%
clf
clear emg_Lab_tally emg_Rab_tally emg_Llum_tally emg_Rlum_tally
clear emg_Lglut_tally emg_Rglut_tally emg_Lham_tally emg_Rham_tally
for i=0:tot_cycs-2
  emg_Lab_tally(i+1,:) =
emg_Lab(start_cyce+i*ave_cyc_Le:start_cyce+(i+1)*ave_cyc_Le-1);
  emg_Rab_tally(i+1,:) =
emg_Rab(start_cyce+i*ave_cyc_Le:start_cyce+(i+1)*ave_cyc_Le-1);
  emg_Llum_tally(i+1,:) =
emg_Llum(start_cyce+i*ave_cyc_Le:start_cyce+(i+1)*ave_cyc_Le-1);
  emg_Rlum_tally(i+1,:) =
emg_Rlum(start_cyce+i*ave_cyc_Le:start_cyce+(i+1)*ave_cyc_Le-1);
  emg_Lglut_tally(i+1,:) =
emg_Lglut(start_cyce+i*ave_cyc_Le:start_cyce+(i+1)*ave_cyc_Le-1);
  emg_Rglut_tally(i+1,:) =
emg_Rglut(start_cyce+i*ave_cyc_Le:start_cyce+(i+1)*ave_cyc_Le-1);
```

```
  emg_Lham_tally(i+1,:) =
emg_Lham(start_cyce+i*ave_cyc_Le:start_cyce+(i+1)*ave_cyc_Le-1);
  emg_Rham_tally(i+1,:) =
emg_Rham(start_cyce+i*ave_cyc_Le:start_cyce+(i+1)*ave_cyc_Le-1);
end

memgLab = mean(emg_Lab_tally,1);
   semgLab = std(emg_Lab_tally);
memgRab = mean(emg_Rab_tally,1);
   semgRab = std(emg_Rab_tally);

memgLlum = mean(emg_Llum_tally,1);
   semgLlum = std(emg_Llum_tally);
memgRlum = mean(emg_Rlum_tally,1);
   semgRlum = std(emg_Rlum_tally);

memgLglut = mean(emg_Lglut_tally,1);
   semgLglut = std(emg_Lglut_tally);
memgRglut = mean(emg_Rglut_tally,1);
   semgRglut = std(emg_Rglut_tally);

memgLham = mean(emg_Lham_tally,1);
   semgLham = std(emg_Lham_tally);
memgRham = mean(emg_Rham_tally,1);
   semgRham = std(emg_Rham_tally);


t_emg = linspace(0,ave_cyc_Le/1500,ave_cyc_Le);

whos t_emg
whos memg1
clf
subplot(421)
plot(t_emg,memgLlum)
title('Llumbar')
subplot(422)
plot(t_emg,memgRlum)
title('Rlumbar')
subplot(425)
plot(t_emg,memgLglut)
title('Lglute')
subplot(426)
plot(t_emg,memgRglut)
title('Rglute')
subplot(423)
plot(t_emg,memgLab)
title('Lab')
subplot(424)
plot(t_emg,memgRab)
title('Rab')

subplot(337)
plot(tk,mHorse_S)
ylabel('Sagittal')
subplot(338)
```

```
plot(tk,mHorse_F)
ylabel('Frontal')
subplot(339)
plot(tk,mHorse_T)
ylabel('Trans')
pause


%% save data here as a .mat file for each participant and test
condition
%Saving Means
data2save.mHorse_F=mHorse_F;
data2save.mHorse_S=mHorse_S;
data2save.mHorse_T=mHorse_T;

data2save.mTrunk_F=mTrunk_F;
data2save.mTrunk_S=mTrunk_S;
data2save.mSho_T=mSho_T;

data2save.mPelvis_F=mPelvis_F;
data2save.mPelvis_S=mPelvis_S;
data2save.mPelvis_T=mPelvis_T;
%Saving Std Dev
data2save.sHorse_F=sHorse_F;
data2save.sHorse_S=sHorse_S;
data2save.sHorse_T=sHorse_T;

data2save.sTrunk_F=sTrunk_F;
data2save.sTrunk_S=sTrunk_S;
data2save.sSho_T=sSho_T;

data2save.sPelvis_F=sPelvis_F;
data2save.sPelvis_S=sPelvis_S;
data2save.sPelvis_T=sPelvis_T;

data2save.EMGLab=memgLab;
data2save.EMGRab=memgRab;
data2save.EMGLlum=memgLlum;
data2save.EMGRlum=memgRlum;
data2save.EMGLglut=memgLglut;
data2save.EMGRglut=memgRglut;
data2save.EMGLham=memgLham;
data2save.EMGRham=memgRham;

% add pelvis roll, yaw, tilt (we have calculated yaw but not roll and
pitch
% for pelvis yet)

%save emg, std across cycles for trunk and pelvis (eg, sTrunk_F)

eval(['Sub',int2str(sub_num),'Ride_TT_',int2str(test_type),'TN',int2str
(test_num),'= data2save'])
eval(['save
Sub',int2str(sub_num),'Ride_TT_',int2str(test_type),'TN',int2str(test_n
um),'
```

```
','Sub',int2str(sub_num),'Ride_TT_',int2str(test_type),'TN',int2str(tes
t_num)])

end
end
end
```

```
%% Summary of Riding data
clear all
close all

sub_it=0;
    for sub=[2,3,4,5,7,8,9,10,11] %enter in participant numbers here
(I'm repeating participant 2 just as a filler)
    sub_it=sub_it+1;
    dummy=0;
    for test_type=[1:2]
        if test_type==1
            test_num_tally=[1:3];
        else
             test_num_tally=[1:5]; %typically make this 1:5
        end

     for test_num=test_num_tally
         dummy=dummy+1;
    eval(['load
Sub',int2str(sub),'Ride_TT_',int2str(test_type),'TN',int2str(test_num),
';']); %all data

eval(['data_temp=Sub',int2str(sub),'Ride_TT_',int2str(test_type),'TN',i
nt2str(test_num),';']); %all data

%row=participant, column=data, dummy=test condition
mTrunk_F(sub_it,:,dummy) = data_temp.mTrunk_F; %trunk sway
vel_mTrunk_F(sub_it,:,dummy) = cdiff(data_temp.mTrunk_F)*120; %velocity
sTrunk_F(sub_it,:,dummy) = data_temp.sTrunk_F;
mTrunk_S(sub_it,:,dummy) = data_temp.mTrunk_S;
sTrunk_S(sub_it,:,dummy) = data_temp.sTrunk_S;
mPelvis_F(sub_it,:,dummy) = data_temp.mPelvis_F;
sPelvis_F(sub_it,:,dummy) = data_temp.sPelvis_F;
mSho_T(sub_it,:,dummy) = data_temp.mSho_T;
sSho_T(sub_it,:,dummy) = data_temp.sSho_T;
mHorse_F(sub_it,:,dummy) = data_temp.mHorse_F;
mHorse_S(sub_it,:,dummy) = data_temp.mHorse_S;
mHorse_T(sub_it,:,dummy) = data_temp.mHorse_T;

EMGLlum(sub_it,:,dummy) = (data_temp.EMGLlum);
EMGRlum(sub_it,:,dummy) = (data_temp.EMGRlum);
EMGLglut(sub_it,:,dummy) = (data_temp.EMGLglut);
EMGRglut(sub_it,:,dummy) = (data_temp.EMGRglut);
EMGLab(sub_it,:,dummy) = (data_temp.EMGLab);
EMGRab(sub_it,:,dummy) = (data_temp.EMGRab);
    end
    end
    end


    %% Plots of INDIVIDUAL participants
    t_vec=linspace(0,205/120-1/120,205);
for i=1:3 %should be 1:8
```

```
    for sub=1:9 %number of participants
subplot(3,3,i)
plot(t_vec,mTrunk_F(sub,:,i),'LineWidth',2); hold on
%plot(t_vec,mTrunk_F(sub,:,i)+sTrunk_F(sub,:,i),'LineWidth',.5,'Color',
[.1 .0 0])
%plot(t_vec,mTrunk_F(sub,:,i)-
sTrunk_F(sub,:,i),'LineWidth',.5,'Color',[.1 .0 0])
ylim([-8 8])
title(['C7 frontal'])
grid on
    end
end
pause
clf

for i=1:3
   for sub=1:9 %number of participants
subplot(3,3,i)
plot(t_vec,mTrunk_S(sub,:,i),'LineWidth',2); hold on
%plot(t_vec,mTrunk_S(sub,:,i)+sTrunk_S(sub,:,i),'LineWidth',.5,'Color',
[.1 .0 0])
%plot(t_vec,mTrunk_S(sub,:,i)-
sTrunk_S(sub,:,i),'LineWidth',.5,'Color',[.1 .0 0])
ylim([-8 8])
title(['C7 saggittal'])
grid on
   end
end
pause


%% Take averages across participants
%Find average trunk sway for each test condition
mmTrunk_f=[];
msTrunk_F=[];
mmTrunk_S=[];
msTrunk_S=[];
mvel_mTrunkF=[];
mmSho_T=[];
mmHorse_F=[];
mmHorse_S=[];
mmHorse_R=[];
msSho_T=[];
stdmSho_T=[];
stdmTrunk_S=[];

for i=1:3 %should be 1:8
mmTrunk_F(i,:)=mean(mTrunk_F(:,:,i)); %mean participant for average
cycle
msTrunk_F(i,:)=mean(sTrunk_F(:,:,i)); %mean std across cycles
stdmTrunk_F(i,:)=std(mTrunk_F(:,:,i)); %std across participants for one
cycle
mvel_mTrunkF(i,:)=mean(vel_mTrunk_F(:,:,i)); %vel mean participant for
average cycle

mmTrunk_S(i,:)=mean(mTrunk_S(:,:,i));
```

```
msTrunk_S(i,:)=mean(sTrunk_S(:,:,i));
stdmTrunk_S(i,:)=std(mTrunk_S(:,:,i)); %std across participants for one
cycle

mmSho_T(i,:)=mean(mSho_T(:,:,i));
msSho_T(i,:)=mean(sSho_T(:,:,i));
stdmSho_T(i,:)=std(mSho_T(:,:,i)); %std across participants for one
cycle

mmHorse_F(i,:)=mean(mHorse_F(:,:,i));
mmHorse_S(i,:)=mean(mHorse_S(:,:,i));
mmHorse_T(i,:)=mean(mHorse_T(:,:,i));
end
```

```
%% Plots of AVERAGE participant
close all
    t_vec=linspace(0,205/120-1/120,205);
for i=1:3 %should be 1:8
figure(1)
subplot(3,1,i)
plot(t_vec,mmTrunk_F(i,:),'b','LineWidth',2); hold on
plot(t_vec,mmTrunk_F(i,:)+stdmTrunk_F(i,:),'LineWidth',.5,'Color',[.1
.0 0])
plot(t_vec,mmTrunk_F(i,:)-stdmTrunk_F(i,:),'LineWidth',.5,'Color',[.1
.0 0])
ylim([-8 8])
title(['Trunk frontal'])
grid on

figure(2)
subplot(3,1,i)
plot(t_vec,mmTrunk_S(i,:),'b','LineWidth',2); hold on
plot(t_vec,mmTrunk_S(i,:)+stdmTrunk_S(i,:),'LineWidth',.5,'Color',[.1
.0 0])
plot(t_vec,mmTrunk_S(i,:)-stdmTrunk_S(i,:),'LineWidth',.5,'Color',[.1
.0 0])
ylim([-8 8])
title(['Trunk sag'])
grid on

figure(3)
subplot(3,1,i)
plot(t_vec,mmSho_T(i,:),'b','LineWidth',2); hold on
plot(t_vec,mmSho_T(i,:)+stdmSho_T(i,:),'LineWidth',.5,'Color',[.1 .0
0])
plot(t_vec,mmSho_T(i,:)-stdmSho_T(i,:),'LineWidth',.5,'Color',[.1 .0
0])
ylim([-8 8])
title(['Trunk trans'])
grid on
```

```
end
pause
close all



%% Tabulate metrics (averages across trials)
subplot(231)
bar([1:3],max(mmTrunk_F,[],2)-min(mmTrunk_F,[],2))
title('trunk c7 fron')

subplot(232)
bar([1:3],max(mmTrunk_S,[],2)-min(mmTrunk_S,[],2))
title('trunk c7 sag')

subplot(233)
bar([1:3],max(mmSho_T,[],2)-min(mmSho_T,[],2))
title('trunk c7 trans')

subplot(234)
bar([1:3],mean(msTrunk_F,2))
title('trunk c7 fron std')

subplot(235)
bar([1:3],mean(msTrunk_S,2))
title('trunk c7 sag std')

subplot(236)
bar([1:3],mean(msSho_T,2))
title('trunk c7 trans std')

pause
clf

% mmTrunk_F;
% mmTrunk_S;
% mmSho_T;
% f = mean(msTrunk_F)
% s = mean(msTrunk_S)
% t = mean(msSho_T)


%% Frequency domain on AVERAGE participant
clf
for i=1:8 % do all test conditions
subplot(431)
[y_tf,f]=dft(mmTrunk_F(i,:)',120,20);
stem(f,abs(y_tf),'b'); hold on
set(gca,'xscal','log')
xlim([0.3 8])
title(['trunk C7 fr ','testnum=',int2str(i)])
ylabel('deg')
```

```
subplot(432)
[y_ts,f]=dft(mmTrunk_S(i,:)',120,20);
stem(f,abs(y_ts),'r')
set(gca,'xscal','log')
xlim([0.3 8])
title('trunk C7 sag')
ylabel('deg')

subplot(433)
[y_tt,f]=dft(mmSho_T(i,:)',120,20);
stem(f,abs(y_tt),'g')
set(gca,'xscal','log')
xlim([0.3 8])
title('trunk C7 trans')
ylabel('deg')

subplot(434)
[y_hf,f]=dft(mmHorse_F(i,:)',120,20);
stem(f,abs(y_hf),'b'); hold on
set(gca,'xscal','log')
xlim([0.3 8])
title('horse fron')
ylabel('deg')

subplot(435)
[y_hs,f]=dft(mmHorse_S(i,:)',120,20);
stem(f,abs(y_hs),'r')
set(gca,'xscal','log')
xlim([0.3 8])
title('horse sag')
ylabel('deg')

subplot(436)
[y_ht,f]=dft(mmHorse_T(i,:)',120,20);
stem(f,abs(y_ht),'g')
xlim([0.1 5])
set(gca,'xscal','log')
xlim([0.3 8])
title('horse trans')
ylabel('deg')

% here is a code to calculate gain and phase a frequencies
% where the horse motion is > 0.2 deg (arbitrary but reasonable)

%frontal plane
mag_hf=[];
pha_hf=[];
iii=0;
for ii=[1,3]
        iii=iii+1;
        f_hf(iii)=f(ii);
        mag_hf(iii)=abs(y_tf(ii)/y_hf(ii));
        pha_hf(iii)=180/pi*angle(y_tf(ii)/y_hf(ii));
end
subplot(437)
stem(f_hf,mag_hf,'b')
```

```
set(gca,'xscal','log')
xlim([0.3 8])
subplot(4,3,10)
stem(f_hf,pha_hf,'b')
set(gca,'xscal','log')
xlim([0.3 8])

%saggital plane
mag_hs=[];
pha_hs=[];
iii=0;
for ii=[2,4]
        iii=iii+1;
        f_hs(iii)=f(ii);
        mag_hs(iii)=abs(y_ts(ii)/y_hs(ii));
        pha_hs(iii)=180/pi*angle(y_ts(ii)/y_hs(ii));
end
subplot(438)
stem(f_hs,mag_hs,'r')
set(gca,'xscal','log')
xlim([0.3 8])
subplot(4,3,11)
stem(f_hs,pha_hs,'r')
set(gca,'xscal','log')
xlim([0.3 8])

%transverse plane
mag_ht=[];
pha_ht=[];
iii=0;
for ii=[1,3]
        iii=iii+1;
        f_ht(iii)=f(ii);
        mag_ht(iii)=abs(y_tt(ii)/y_ht(ii));
        pha_ht(iii)=180/pi*angle(y_tt(ii)/y_ht(ii));
end
subplot(439)
stem(f_ht,mag_ht,'g')
set(gca,'xscal','log')
xlim([0.3 8])
subplot(4,3,12)
stem(f_ht,pha_ht,'g')
set(gca,'xscal','log')
xlim([0.3 8])

pause
clf

end
%% Now look at EMG
clf
load balance
clear arEMGLab arEMGRab arEMGLlum arEMGRlum arEMGLglut arEMGRglut
for kk=1:sub_it %put in total number of participants here
   for ii=1:3
subplot(231)
```

```
plot(EMGLab(kk,:,ii))
title(['s',int2str(kk),'test= ',int2str(ii)])
subplot(232)
plot(EMGRab(kk,:,ii))
subplot(233)
plot(EMGLlum(kk,:,ii))
subplot(234)
plot(EMGRlum(kk,:,ii))
subplot(235)
plot(EMGLglut(kk,:,ii))
subplot(236)
plot(EMGRglut(kk,:,ii))

arEMGLab(ii,kk)=mean(EMGLab(kk,:,ii),2);
arEMGRab(ii,kk)=mean(EMGRab(kk,:,ii),2);
arEMGLlum(ii,kk)=mean(EMGLlum(kk,:,ii),2);
arEMGRlum(ii,kk)=mean(EMGRlum(kk,:,ii),2);
arEMGLglut(ii,kk)=mean(EMGLglut(kk,:,ii),2);
arEMGRglut(ii,kk)=mean(EMGRglut(kk,:,ii),2);

pause
    end
end
```

APPENDIX B

Sample Raw Electromyography Data

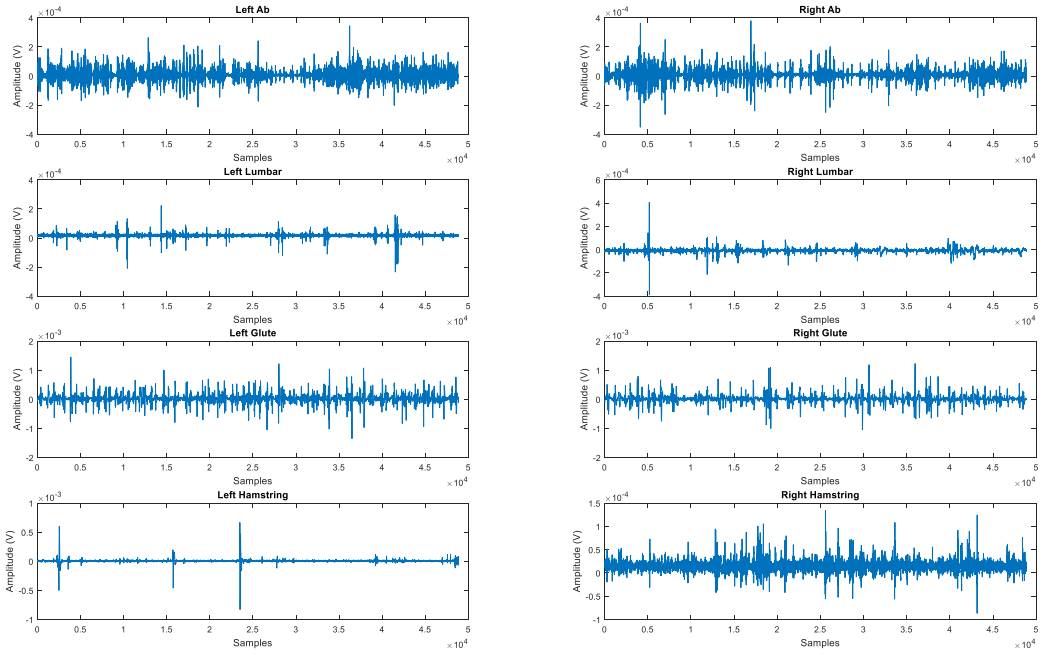

B.1: First 30 seconds of Riding for Participant 8

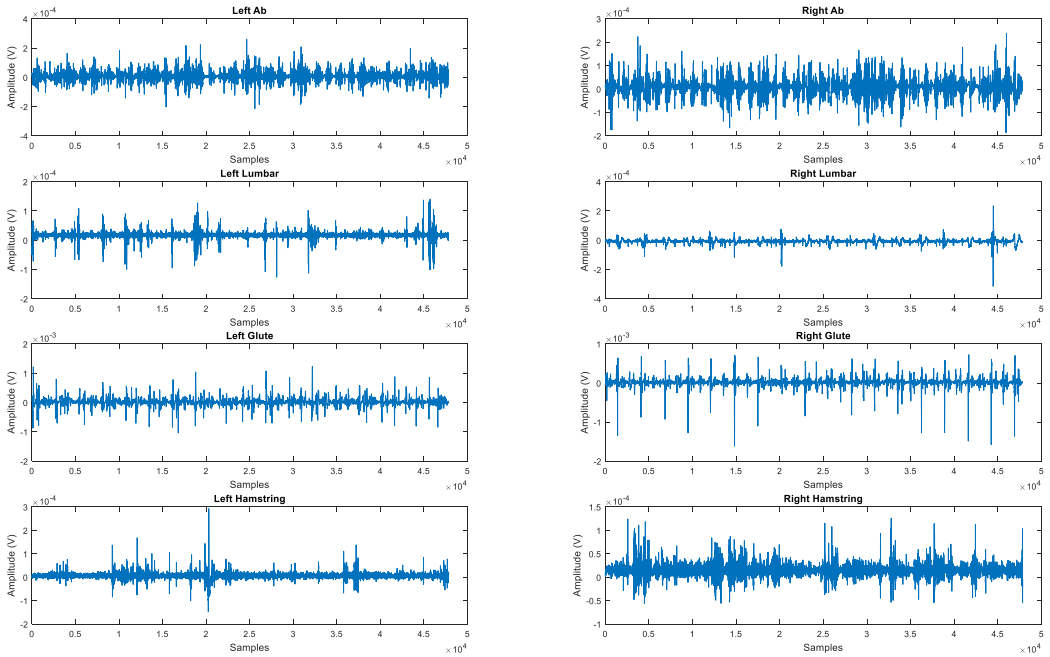

B.2: Middle 30 seconds of Riding for Participant 8

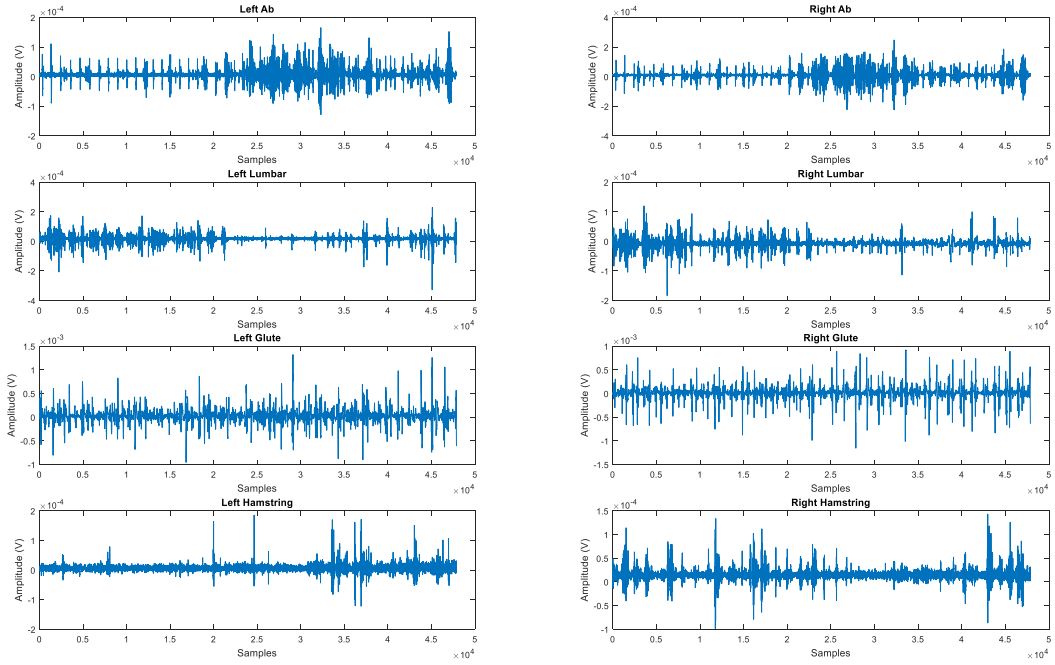

B.3: Final 30 seconds of Riding for Participant 8

APPENDIX C

Pre and Post-Ride Alternating Hip Extension EMG Data

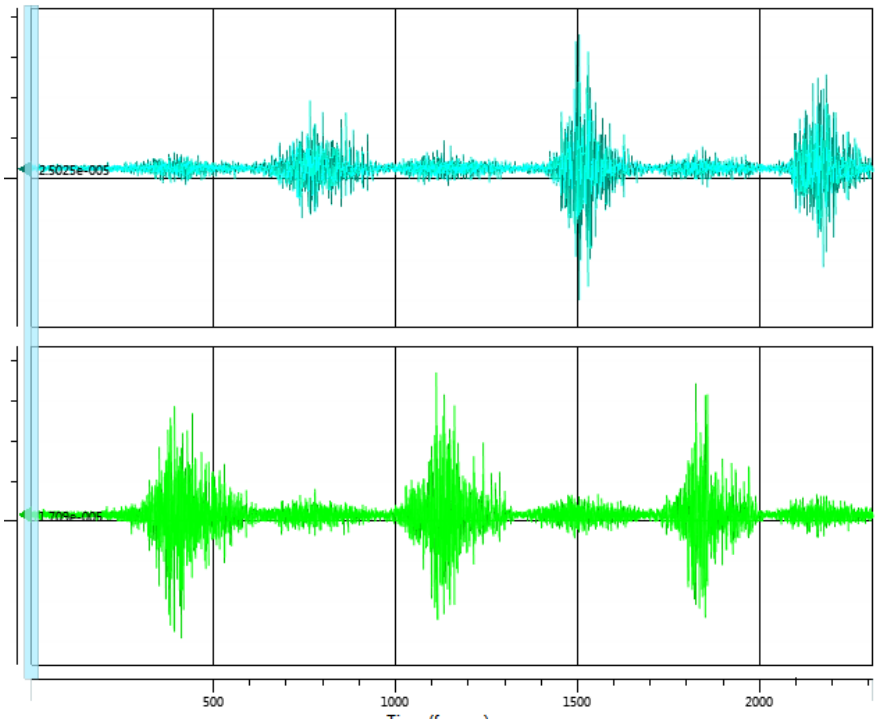

C.1: Pre-Ride Alternating Hip Extension

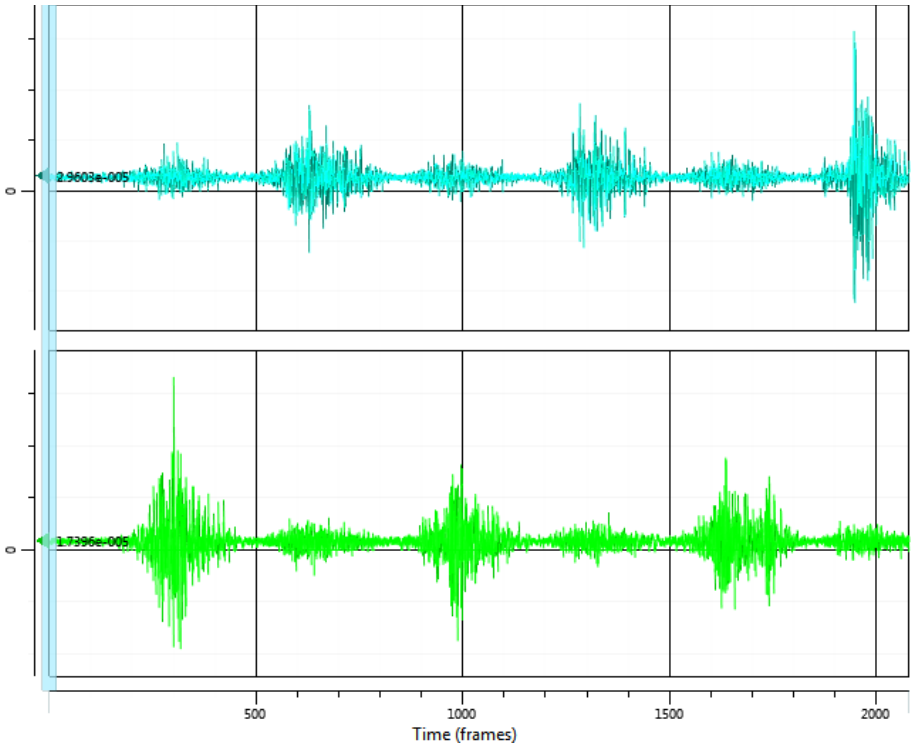

C.2: Post-Ride1 Alternating Hip Extension

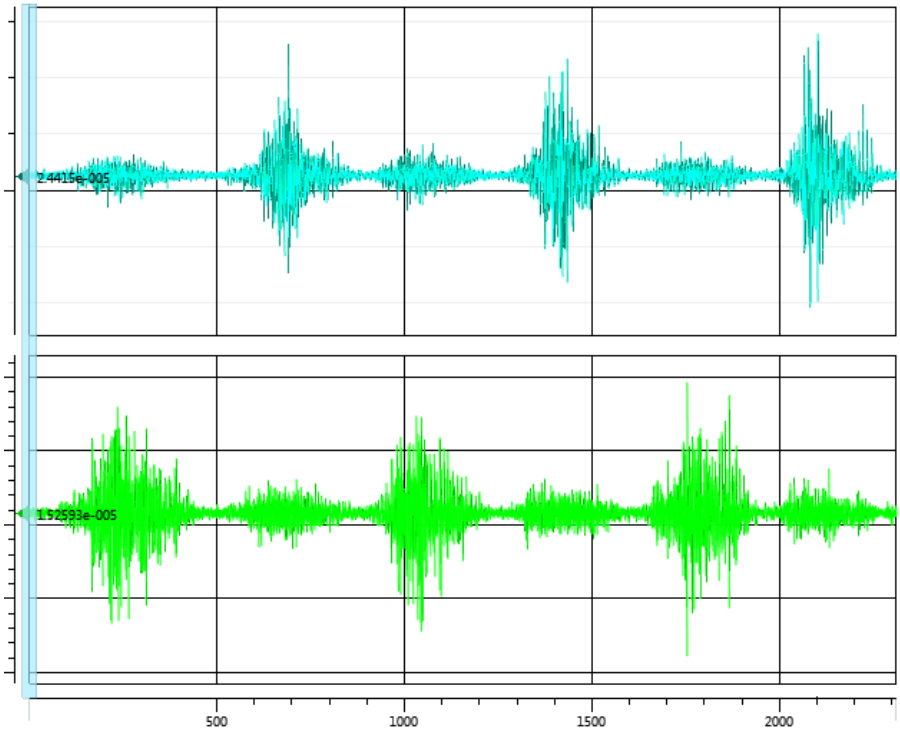

C.3: Post-Ride2 Alternating Hip Extension

APPENDIX D

Balance Test Measures For All Participants

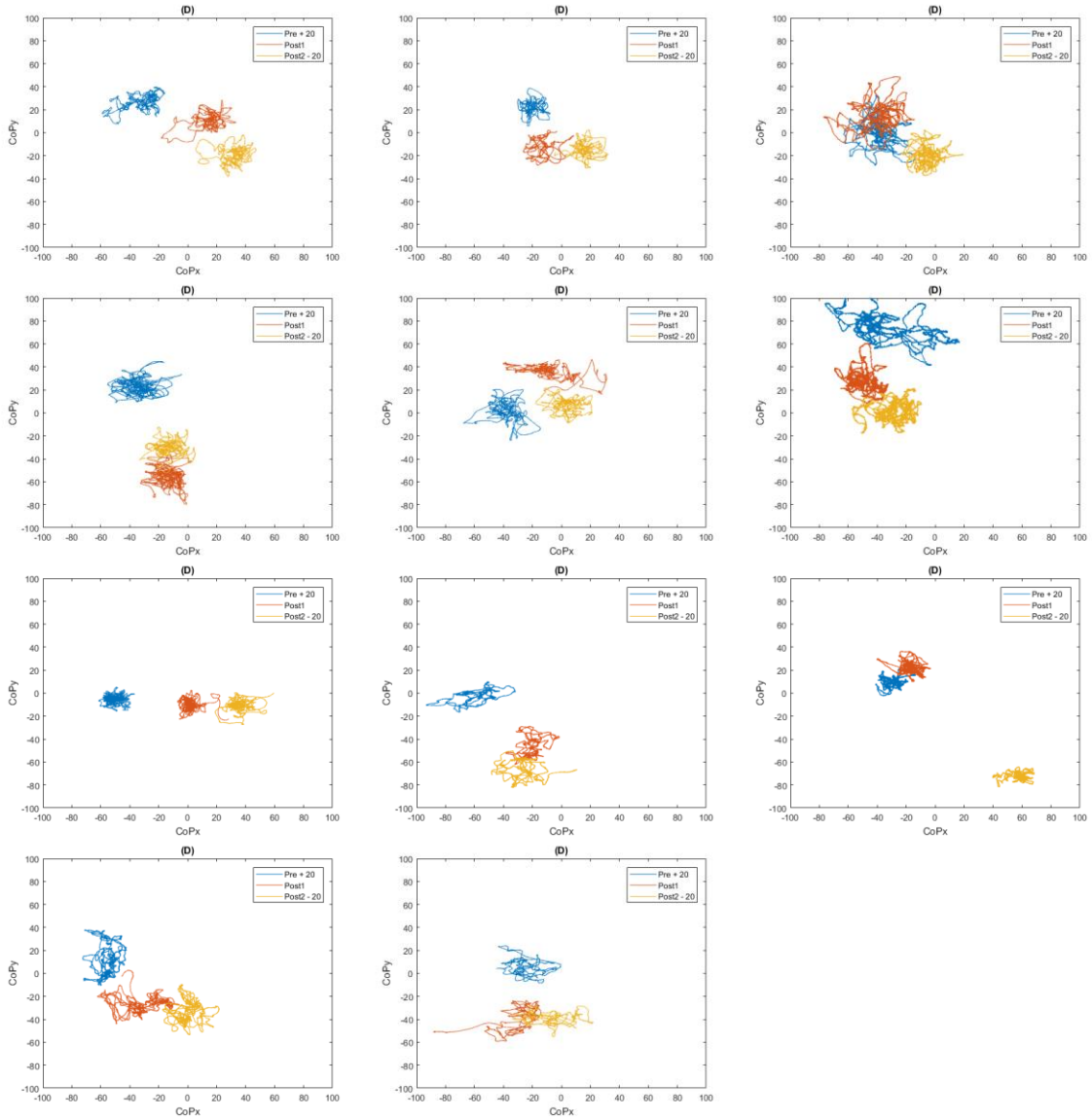

D.1: Closed Eye, Two-Legged Balance CoPy vs. CoPx for all participants. Blue is the pre-ride balance test, the red is the first post-ride test, and the yellow is the second post-ride test.

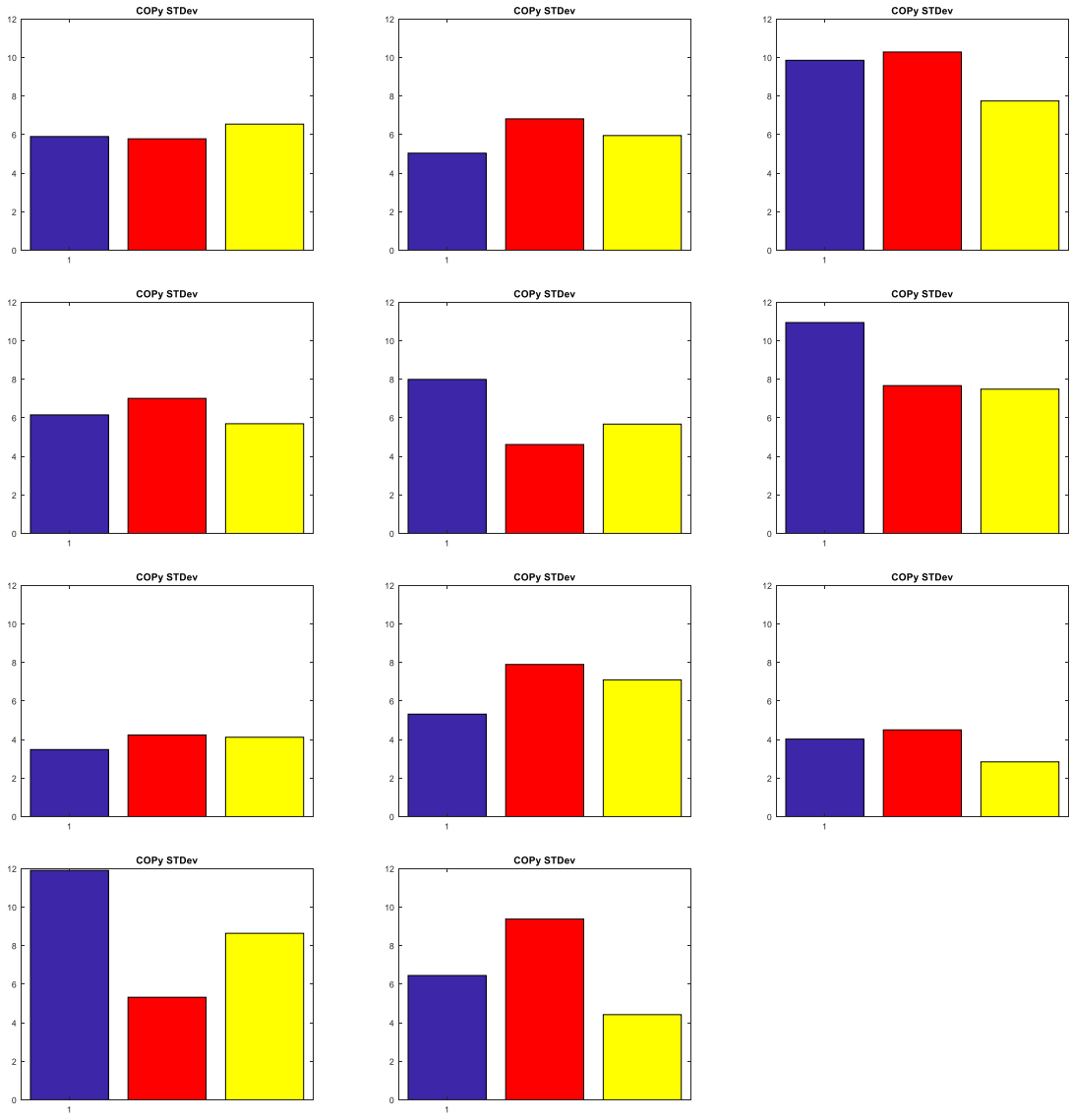

D.2: CoPy standard deviations of each participant across three closed eye, two-legged balance tests. Blue is the pre-ride balance test, the red is the first post-ride test, and the yellow is the second post-ride test.

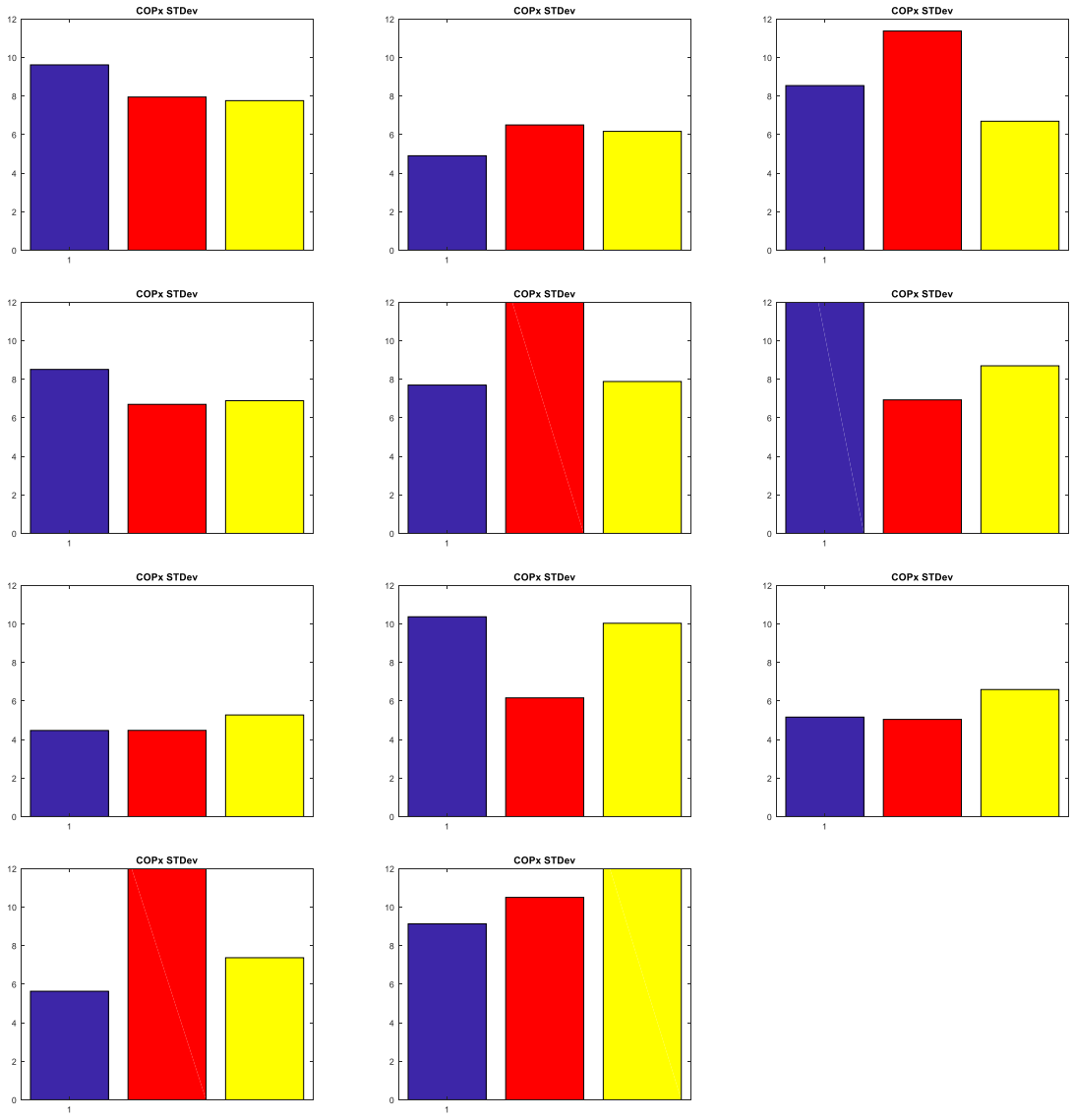

D.3: CoPx standard deviations of each participant across three closed eye, two-legged balance tests. Blue is the pre-ride balance test, the red is the first post-ride test, and the yellow is the second post-ride test.

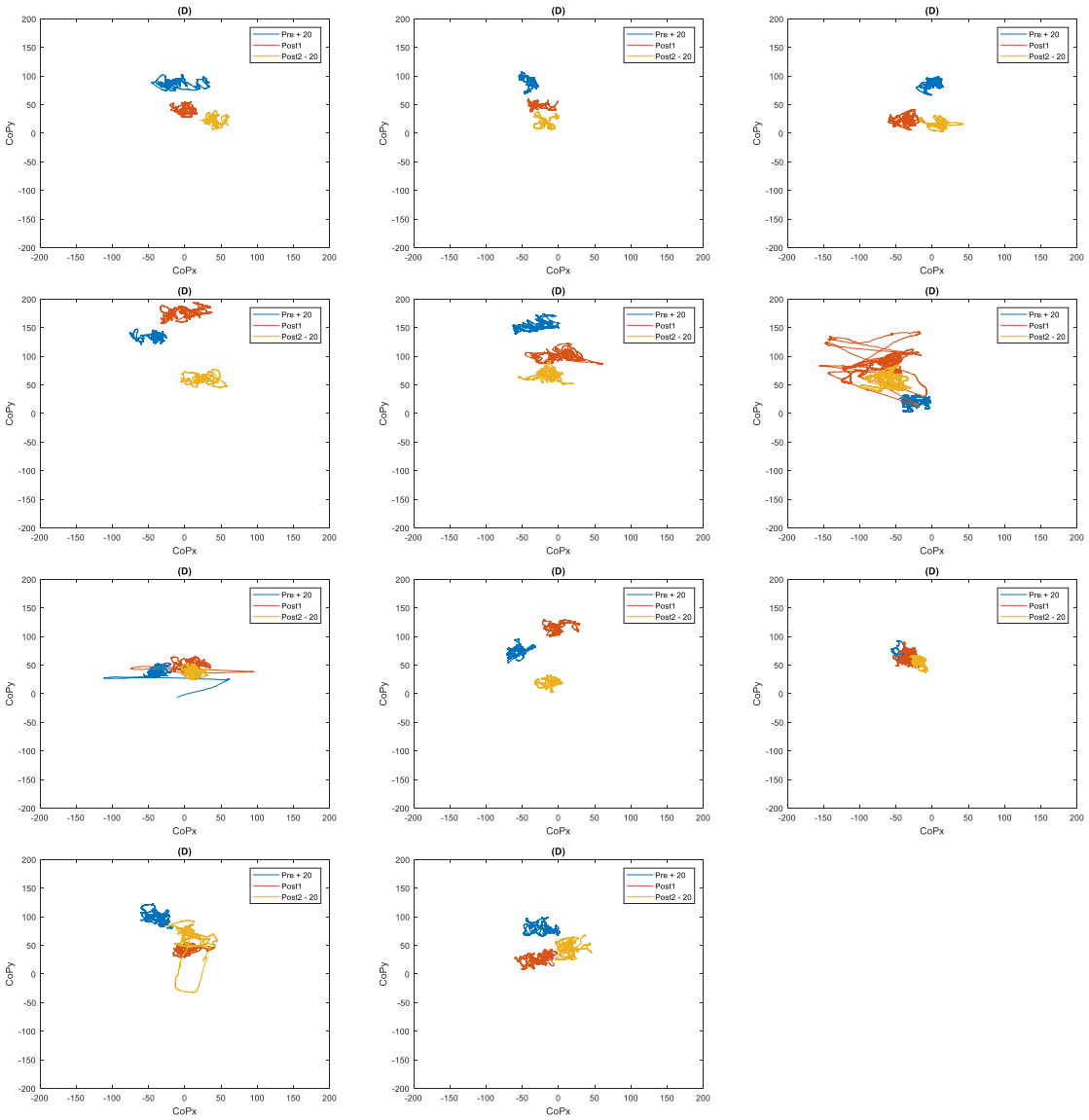

D.4: Left Leg Balance CoPy vs. CoPx for all participants

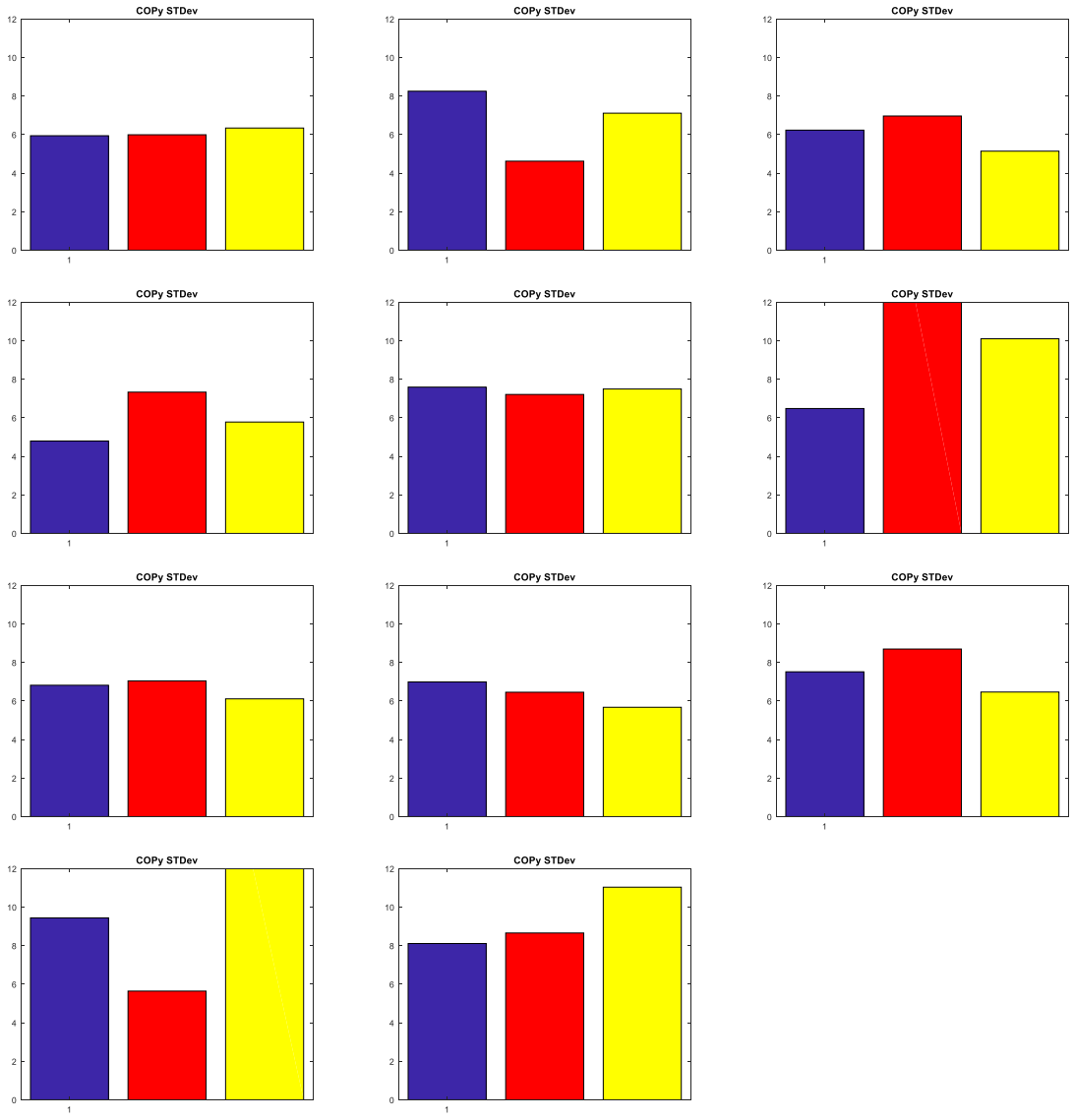

D.5: CoPy standard deviations of each participant across three left leg balance tests. Blue is the pre-ride balance test, the red is the first post-ride test, and the yellow is the second post-ride test.

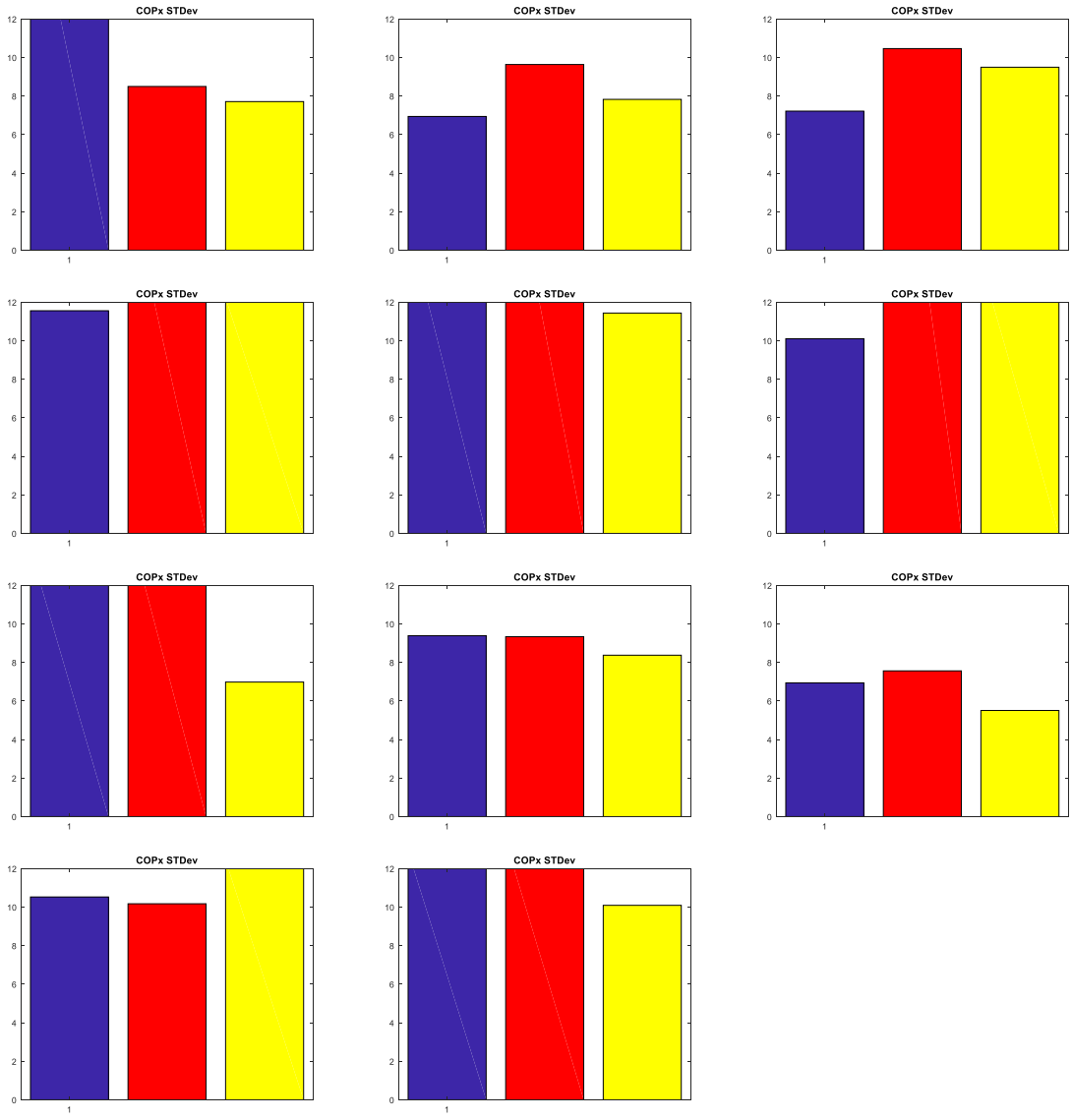

D.6: CoPx standard deviations of each participant across three left leg balance tests. Blue is the pre-ride balance test, the red is the first post-ride test, and the yellow is the second post-ride test.

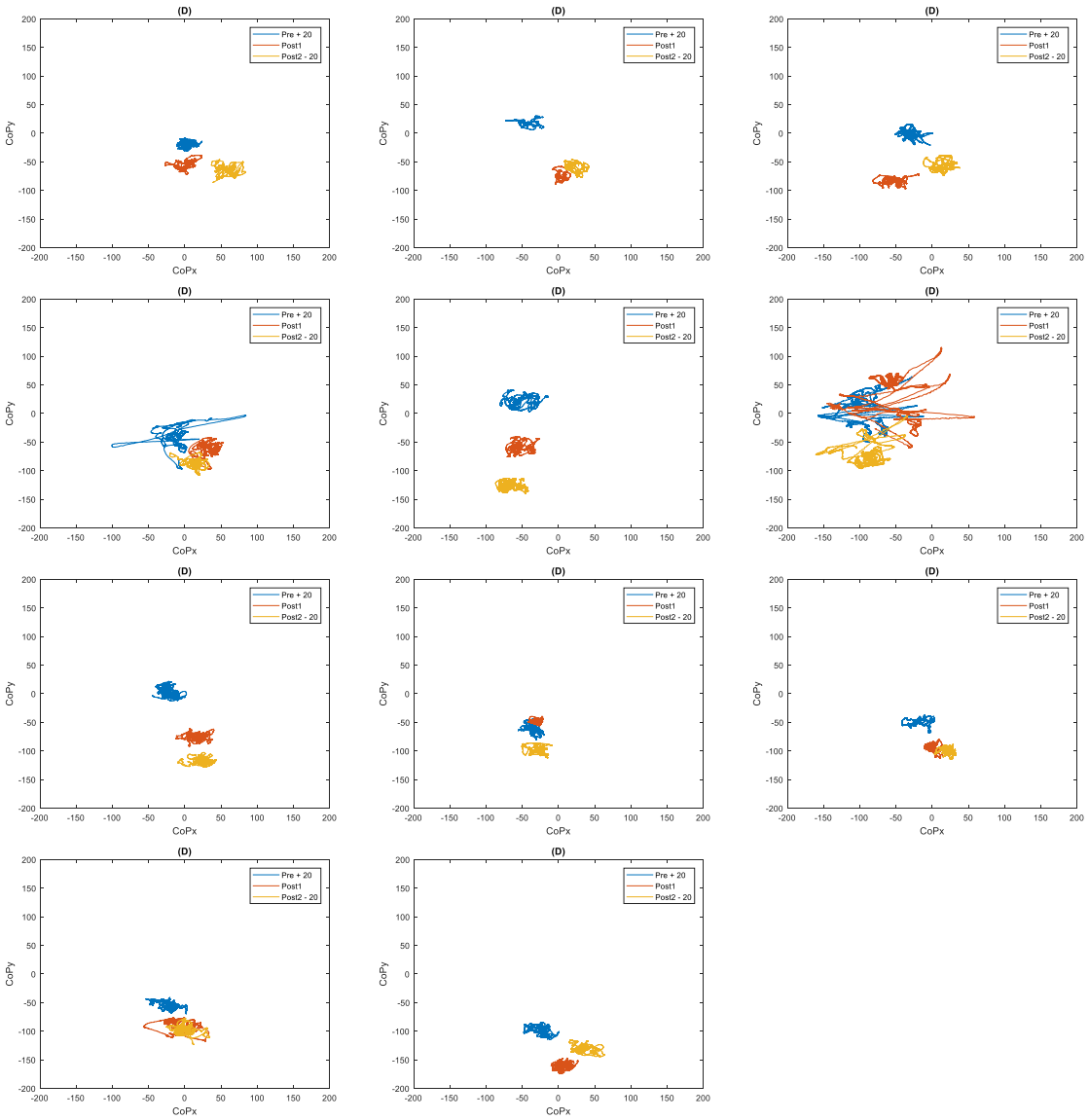

D.7: Right Leg Balance CoPy vs. CoPx for all participants

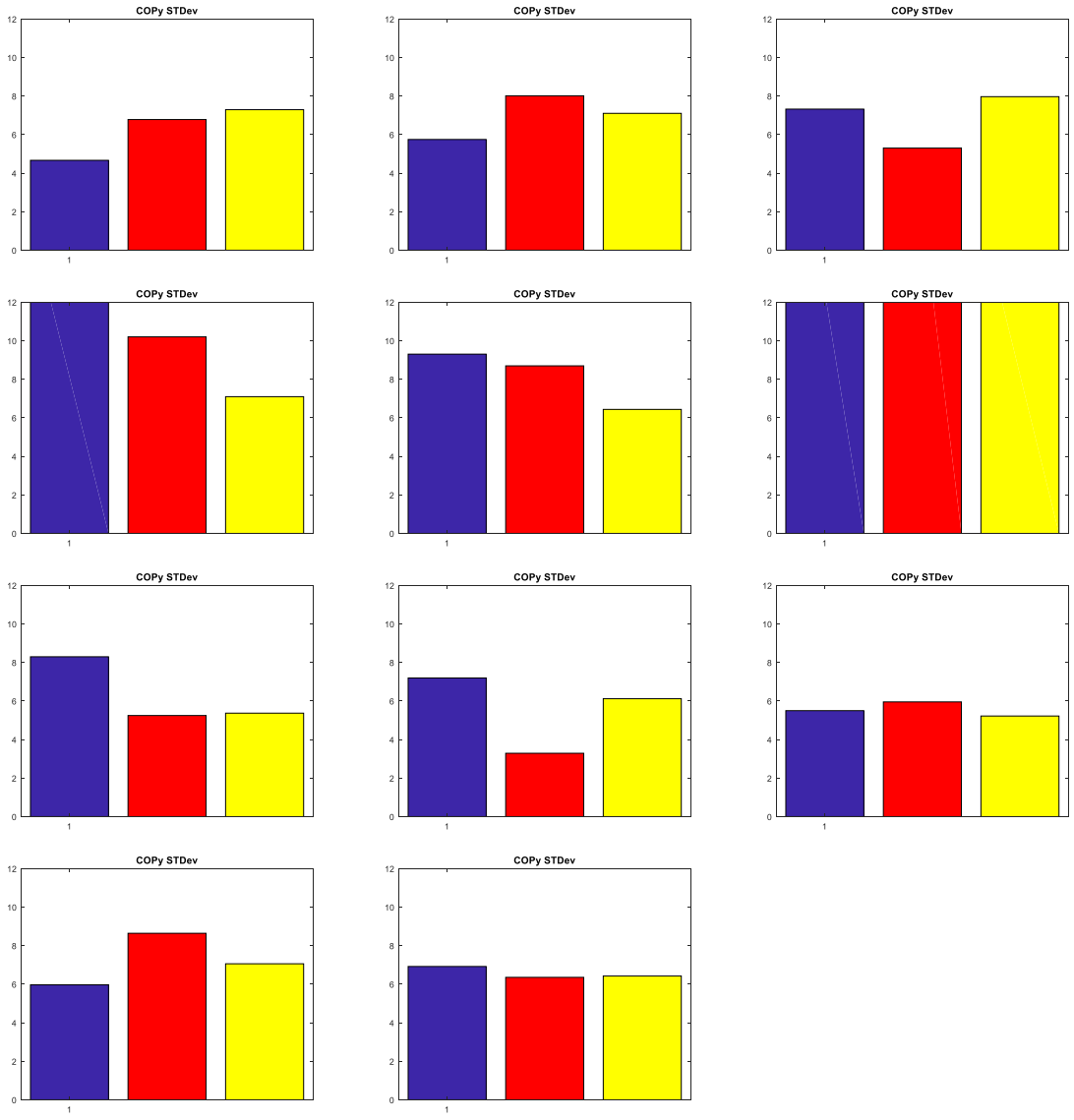

D.8: CoPy standard deviations of each participant across three right leg balance tests. Blue is the pre-ride balance test, the red is the first post-ride test, and the yellow is the second post-ride test.

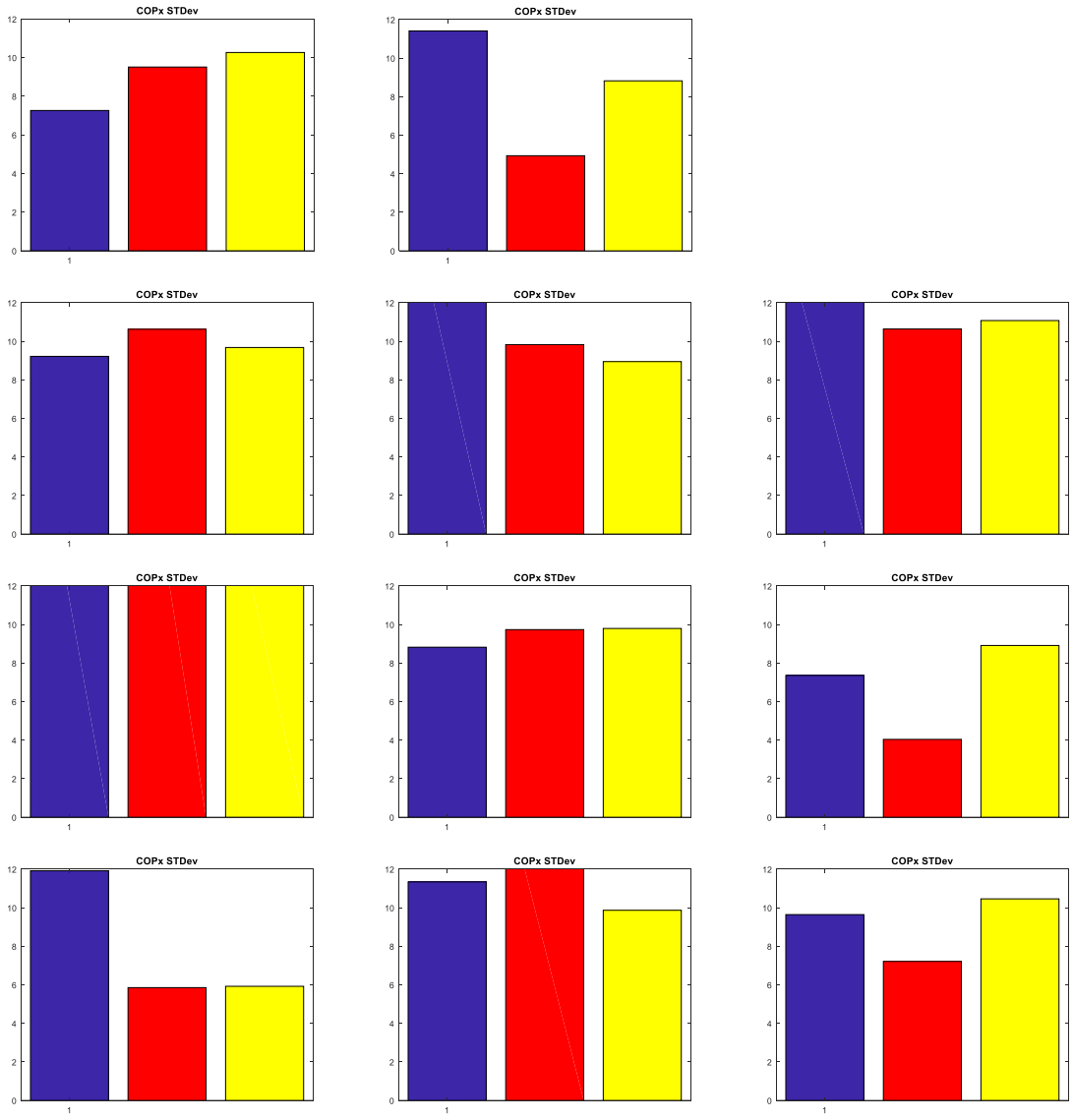

D.9: CoPx standard deviations of each participant across three right leg balance tests. Blue is the pre-ride balance test, the red is the first post-ride test, and the yellow is the second post-ride test.

BIBLIOGRAPHY

[1] Lee, C.-W., Kim, S. G., and Yong, M. S., 2014, "Effects of Hippotherapy on Recovery of Gait and Balance Ability in Patients with Stroke," J. Phys. Ther. Sci., **26**(2), pp. 309–311.

[2] Casady, R. L., and Nichols-Larsen, D. S., 2004, "The Effect of Hippotherapy on Ten Children with Cerebral Palsy," Pediatr. Phys. Ther., **16**(3), p. 165.

[3] Sterba, J. A., 2007, "Does Horseback Riding Therapy or Therapist-Directed Hippotherapy Rehabilitate Children with Cerebral Palsy?," Dev. Med. Child Neurol., **49**(1), pp. 68–73.

[4] Meregillano, G., 2004, "Hippotherapy," Phys. Med. Rehabil. Clin., **15**(4), pp. 843–854.

[5] Garner, B. A., and Rigby, B. R., 2015, "Human Pelvis Motions When Walking and When Riding a Therapeutic Horse," Hum. Mov. Sci., **39**, pp. 121–137.

[6] CDC, 2017, "CDC Works 24/7," Cent. Dis. Control Prev. [Online]. Available: https://www.cdc.gov/index.htm. [Accessed: 27-Feb-2018].

[7] "NSIP - Basic Facts: People with Disabilities" [Online]. Available: http://www.serviceandinclusion.org/index.php?page=basic. [Accessed: 10-Mar-2018].

[8] "National Institutes of Health (NIH)," Natl. Inst. Health NIH [Online]. Available: https://www.nih.gov/. [Accessed: 27-Feb-2018].

[9] Fugl-Meyer, A. R., Jääskö, L., Leyman, I., Olsson, S., and Steglind, S., 1975, "The Post-Stroke Hemiplegic Patient. 1. a Method for Evaluation of Physical Performance.," Scand. J. Rehabil. Med., **7**(1), pp. 13–31.

[10] "United Cerebral Palsy."

[11] "Classification of Gait Patterns in Cerebral Palsy - Physiopedia" [Online]. Available: https://www.physio-pedia.com/Classification_of_Gait_Patterns_in_Cerebral_Palsy. [Accessed: 14-Mar-2018].

[12] "What Are the Treatments for Spinal Cord Injury (SCI)?," http://www.nichd.nih.gov/ [Online]. Available: http://www.nichd.nih.gov/health/topics/spinalinjury/conditioninfo/treatments. [Accessed: 12-Mar-2018].

[13] Peterka, R. J., 2002, "Sensorimotor Integration in Human Postural Control," J. Neurophysiol., **88**(3), pp. 1097–1118.

[14] Berthoz, A., Lacour, M., Soechting, J. F., and Vidal, P. P., 1979, "The Role of Vision in the Control of Posture During Linear Motion," *Progress in Brain Research*, R. Granit, and O. Pompeiano, eds., Elsevier, pp. 197–209.

[15] Allum, J. H. J., and Pfaltz, C. R., 1983, "Influence of Bilateral and Acute Unilateral Peripheral Vestibular Deficits on Early Sway Stabilizing Responses in Human Tibialis Anterior Muscles," Acta Otolaryngol. (Stockh.), **96**(sup406), pp. 115–119.

[16] Hlavacka, F., and Njiokiktjien, C., 1985, "Postural Responses Evoked by Sinusoidal Galvanic Stimulation of the Labyrinth: Influence of Head Position," Acta Otolaryngol. (Stockh.), **99**(1–2), pp. 107–112.

[17] Horak, F. B., 2006, "Postural Orientation and Equilibrium: What Do We Need to Know about Neural Control of Balance to Prevent Falls?," Age Ageing, **35**(suppl_2), pp. ii7–ii11.

[18] Agrawal, Y., Carey, J. P., Santina, C. C. D., Schubert, M. C., and Minor, L. B., 2009, "Disorders of Balance and Vestibular Function in US Adults: Data From the National Health and Nutrition Examination Survey, 2001-2004," Arch. Intern. Med., **169**(10), pp. 938–944.

[19] Mansfield, A., Aqui, A., Centen, A., Danells, C. J., DePaul, V. G., Knorr, S., Schinkel-Ivy, A., Brooks, D., Inness, E. L., McIlroy, W. E., and Mochizuki, G., 2015, "Perturbation Training to Promote Safe Independent Mobility Post-Stroke: Study Protocol for a Randomized Controlled Trial," BMC Neurol., **15**.

[20] 2011, "The Human Balance System," Vestib. Disord. Assoc. [Online]. Available: http://vestibular.org/understanding-vestibular-disorder/human-balance-system. [Accessed: 02-Mar-2018].

[21] Goodworth, A. D., Paquette, C., Jones, G. M., Block, E. W., Fletcher, W. A., Hu, B., and Horak, F. B., 2012, "Linear and Angular Control of Circular Walking in Healthy Older Adults and Subjects with Cerebellar Ataxia," Exp. Brain Res., **219**(1), pp. 151–161.

[22] Hallberg, L., 2008, *Walking the Way of the Horse: Exploring the Power of the Horse-Human Relationship*, iUniverse.

[23] Whalen, C. N., and Case-Smith, J., 2012, “Therapeutic Effects of Horseback Riding Therapy on Gross Motor Function in Children with Cerebral Palsy: A Systematic Review,” Phys. Occup. Ther. Pediatr., **32**(3), pp. 229–242.

[24] Rigby, B. R., Gloeckner, A. R., Sessums, S., Lanning, B. A., and Grandjean, P. W., 2017, “Changes in Cardiorespiratory Responses and Kinematics With Hippotherapy in Youth With and Without Cerebral Palsy,” Res. Q. Exerc. Sport, **88**(1), pp. 26–35.

[25] Mackay-Lyons, M., Conway, C., and Roberts, W., 1988, “Effects of Therapeutic Riding on Patients with Multiple Sclerosis: A Preliminary Trial,” Physiother. Can., **40**(2), pp. 104–109.

[26] Han, J. Y., Kim, J. M., Kim, S. K., Chung, J. S., Lee, H.-C., Lim, J. K., Lee, J., and Park, K. Y., 2012, “Therapeutic Effects of Mechanical Horseback Riding on Gait and Balance Ability in Stroke Patients,” Ann. Rehabil. Med., **36**(6), pp. 762–769.

[27] Cho, S.-H., Kim, J.-W., Kim, S.-R., and Cho, B.-J., 2015, “Effects of Horseback Riding Exercise Therapy on Hormone Levels in Elderly Persons,” J. Phys. Ther. Sci., **27**(7), pp. 2271–2273.

[28] Martin, L., Baker, R., and Harvey, A., 2010, “A Systematic Review of Common Physiotherapy Interventions in School-Aged Children with Cerebral Palsy,” Phys. Occup. Ther. Pediatr., **30**(4), pp. 294–312.

[29] van der Krogt, M. M., Sloot, L. H., Buizer, A. I., and Harlaar, J., 2015, “Kinetic Comparison of Walking on a Treadmill versus over Ground in Children with Cerebral Palsy,” J. Biomech. Kidlington, **48**(13), pp. 3586–3592.

[30] Plotnik, M., Azrad, T., Bondi, M., Bahat, Y., Gimmon, Y., Zeilig, G., Inzelberg, R., and Siev-Ner, I., 2015, “Self-Selected Gait Speed - over Ground versus Self-Paced Treadmill Walking, a Solution for a Paradox,” J. NeuroEngineering Rehabil., **12**, p. 20.

[31] “Home,” Always Good Ride [Online]. Available: http://www.alwaysagoodride.com/. [Accessed: 23-Feb-2018].

[32] “The Equicizer | The World’s #1 Mechanical Horse | Equicizer” [Online]. Available: https://equicizer.com/pages/overview. [Accessed: 23-Feb-2018].

[33] Park, J.-H., and You, J. (Sung) H., 2018, “Innovative Robotic Hippotherapy Improves Postural Muscle Size and Postural Stability during the Quiet Stance and Gait Initiation in a Child with Cerebral Palsy: A Single Case Study,” NeuroRehabilitation, **42**(2), pp. 247–253.

[34] Nymark, J. R., Balmer, S. J., Melis, E. H., Lemaire, E. D., and Millar, S., 2005, "Electromyographic and Kinematic Nondisabled Gait Differences at Extremely Slow Overground and Treadmill Walking Speeds," J. Rehabil. Res. Dev. Wash., **42**(4), pp. 523–34.

[35] Dewar, R., Love, S., and Johnston, L. M., 2015, "Exercise Interventions Improve Postural Control in Children with Cerebral Palsy: A Systematic Review," Dev. Med. Child Neurol., **57**(6), pp. 504–520.

[36] Chung, J., Evans, J., Lee, C., Lee, J., Rabbani, Y., Roxborough, L., and Harris, S. R., 2008, "Effectiveness of Adaptive Seating on Sitting Posture and Postural Control in Children with Cerebral Palsy," Pediatr. Phys. Ther., **20**(4), p. 303.

[37] "Normal Weight Ranges: Body Mass Index (BMI)" [Online]. Available: https://www.cancer.org/cancer/cancer-causes/diet-physical-activity/body-weight-and-cancer-risk/adult-bmi.html. [Accessed: 26-Mar-2018].

[38] "A Brief History of Motion Capture for Computer Character Animation" [Online]. Available: https://www.siggraph.org/education/materials/HyperGraph/animation/character_animation/motion_capture/history1.htm. [Accessed: 26-Feb-2018].

[39] Klotz, M. C. M., Kost, L., Braatz, F., Ewerbeck, V., Heitzmann, D., Gantz, S., Dreher, T., and Wolf, S. I., 2013, "Motion Capture of the Upper Extremity during Activities of Daily Living in Patients with Spastic Hemiplegic Cerebral Palsy," Gait Posture, **38**(1), pp. 148–152.

[40] VICON, "VICON," VICON [Online]. Available: https://www.vicon.com/downloads/documentation/plug-in-gait-product-guide. [Accessed: 26-Feb-2018].

[41] Hargrove, L. J., Simon, A. M., Young, A. J., Lipschutz, R. D., Finucane, S. B., Smith, D. G., and Kuiken, T. A., 2013, "Brief Report: Robotic Leg Control with EMG Decoding in an Amputee with Nerve Transfers," N. Engl. J. Med. Boston, **369**(13), pp. 1237–42.

[42] Cifrek, M., Medved, V., Tonković, S., and Ostojić, S., 2009, "Surface EMG Based Muscle Fatigue Evaluation in Biomechanics," Clin. Biomech. Bristol Avon, **24**(4), pp. 327–340.

[43] Carpenter, M. G., Frank, J. S., Silcher, C. P., and Peysar, G. W., 2001, "The Influence of Postural Threat on the Control of Upright Stance," Exp. Brain Res., **138**(2), pp. 210–218.

[44] "Surface EMG," Noraxon USA.

[45] Lehman, G. J., and McGill, S. M., 1999, "The Importance of Normalization in the Interpretation of Surface Electromyography: A Proof of Principle," J. Manipulative Physiol. Ther., **22**(7), pp. 444–446.

[46] De Luca, C. J., 1997, "The Use of Surface Electromyography in Biomechanics," J. Appl. Biomech., **13**(2), pp. 135–163.

[47] Kazamel, M., Province, P., Alsharabati, M., and Oh, S., 2013, "History of Electromyography (EMG) and Nerve Conduction Studies (NCS): A Tribute to the Founding Fathers (P05.259)," Neurology, **80**(7 Supplement), p. P05.259.

[48] "Libby Lamb Illustration" [Online]. Available: http://libbylamb.com/illustration1.html. [Accessed: 11-May-2018].

[49] Goodworth, A. D., and Peterka, R. J., 2009, "Contribution of Sensorimotor Integration to Spinal Stabilization in Humans," J. Neurophysiol., **102**(1), pp. 496–512.

[50] Ruhe, A., Fejer, R., and Walker, B., 2011, "Center of Pressure Excursion as a Measure of Balance Performance in Patients with Non-Specific Low Back Pain Compared to Healthy Controls: A Systematic Review of the Literature," Eur. Spine J., **20**(3), pp. 358–368.

[51] Benoit, H. D., 2011, "Designing, Constructing, and Testing a Second-Generation Prototype Mechanical Hippotherapy Horse.," Thesis.

[52] Kuo, A. D., 1999, "Stabilization of Lateral Motion in Passive Dynamic Walking," Int. J. Robot. Res., **18**(9), pp. 917–930.

[53] McAndrew, P. M., Wilken, J. M., and Dingwell, J. B., 2011, "Dynamic Stability of Human Walking in Visually and Mechanically Destabilizing Environments," J. Biomech., **44**(4), pp. 644–649.

[54] Lee, C.-W., Kim, S. G., and Na, S. S., 2014, "The Effects of Hippotherapy and a Horse Riding Simulator on the Balance of Children with Cerebral Palsy," J. Phys. Ther. Sci., **26**(3), pp. 423–425.

[55] Vogt, L., Portscher, M., Brettmann, K., Pfeifer, K., and Banzer, W., 2003, "Cross-Validation of Marker Configurations to Measure Pelvic Kinematics in Gait," Gait Posture, **18**(3), pp. 178–184.

[56] Vogt, L., Pfeifer, K., Portscher, M., and Banzer, W., 2001, "Influences of Nonspecific Low Back Pain on Three-Dimensional Lumbar Spine Kinematics in Locomotion," Spine, **26**(17), p. 1910.

[57] Janura, M., Peham, C., Dvorakova, T., and Elfmark, M., 2009, “An Assessment of the Pressure Distribution Exerted by a Rider on the Back of a Horse during Hippotherapy,” Hum. Mov. Sci., **28**(3), pp. 387–393.

[58] Muñoz-Lasa, S., Ferriero, G., Valero, R., and Gomez-Muñiz, F., 2011, “Effect of Therapeutic Horseback Riding on Balance and Gait of People with Multiple Sclerosis,” G. Ital. Med. Lav. Ergon., **33**(4), p. 462.